
Addis Ababa University
Addis Ababa Institute of Technology
School of Electrical and Computer Engineering

# Linear Quadratic Gaussian Controller Tuned With Particle Swarm Optimization For Speed Tracking Control of Brushless DC Motor

A thesis submitted to School of Graduate Studies, Addis Ababa Institute of Technology, Addis Ababa University in partial fulfillment of the requirement for the Degree of Master of Science in Electrical Engineering (Control Engineering)

By

Amare Meseret

Advisor

Dr.Dereje Sheferaw

February 12, 2022
Addis Ababa, Ethiopia


Addis Ababa University

Addis Ababa Institute of Technology

School of Electrical and Computer Engineering

# Linear Quadratic Gaussian Controller Tuned With Particle Swarm Optimization For Speed Tracking Control of Brushless DC Motor

By: Amare Meseret

APPROVED BY BOARD OF EXAMINERS

| Name | Signature | Date |
|---|---|---|
| Dr.Bisrat Derebssa (School Dean Person) | ..... | ..... |
| Dr.Dereje Sheferaw (Advisor) | ..... | ..... |
| Dr.Lebsework Negash (Internal Examiner) | ..... | ..... |
| Mr. Getu Gebisa (External Examiner) | ..... | ..... |

# Declaration

I declare that the work entitled "Linear Quadratic Gaussian Controller Tuned With Particle Swarm Optimization For Speed Tracking Control of Brushless DC Motor " is my original work and has not been presented for any degree in this university or any other university or colleges, as well as all sources of material, used for the thesis have been duly acknowledged..

| Name | Signature | Date |
|---|---|---|
| Amare Meseret | ..... | ..... |

# Acknowledgment

First and foremost,I would like to thank my advisors, Dr.Dereje Shiferaw , for their continuing support throughout my MSc studies and research, for their patience, passion, great knowledge, and most importantly, for believing in my potential. Their advice was helpful during the research and writing of my thesis.

Besides my advisor,I would like to extend my thanks of gratitude Dr.Lebsewerk Negash and Dr. Mengesha Mamo for their time dedicated to supervise and review my work and also for their valuable suggestions.
Finally, my thanks go to all the people who have supported me to complete the research work directly or indirectly. Thank you!

Amare Meseret

# Abstract

Brushless DC(BLDC)motors are widely used in Electric Vehicle applications because of their high starting torque, high efficiency, long operating life and better speed versus torque characteristics. The major problem in the brushless dc motor drive system is that some disturbances originate in the drive which will result in errors and reduce the stability of the system. This problem can be fixed by using good modeling approach and high performance controllers like linear quadratic gaussian. But the selection or tuning of the parameters of the linear quadratic gaussian controller is a tedious process. Therefore it is important to use artificial intelligence based optimization methods to select the parameters of the linear quadratic gaussian controllers to achieve the high performance of linear quadratic gaussian controller.

Hence, in this thesis, a linear quadratic gaussian controller tuned with PSO is designed and it's performance in speed control for a Brushless DC motor is analyzed. The performance of the proposed controller of brushless dc motor was analyzed in terms of speed tracking capability, back emf and hall sensor response, high and low-speed behavior, and speed reversal conditions using MATLAB /SIMULINK.

The linear quadratic gaussian controller performance has been compared with proportional integral control strategies in terms of the four quadrants operation and braking system response.The simulation results show that the linear quadratic gaussian-particle swarm optimization controller has a more significant overshoot reduction compared to PI controllers,and a good transient response with a rise time , settling time,and the minimum steady-state speed error percentage of has been achieved for linear quadratic gaussian-particle swarm optimization.Then particle swarm optimization tuned linear quadratic gaussian controller methods are better when compared with PI conventional methods.

Keywords— LQG- PSO, Breaking, Brushless DC Motor,Electrical Vehicle

# Contents

# List of Figures

# List of Tables

# List of Abbreviations

| | |
|---|---|
| AC | Alternating Current |
| BLDC | Brushless Dc Motor |
| DC | Direct Current |
| EKF | Extended Kalman Filter |
| Emf | Electromotive Force |
| EV | Electric Vehicle |
| FLC | Fuzzy Logic Controller |
| HEV | Hybrid Electric Vehicle |
| IGBT | Insulated Gate Bipolar Transistor |
| KVL | Kirchhoff's Voltage Law |
| LQE | Linear Quadratic Estimator |
| LQG | Linear Quadratic Gaussian |
| LQR | Linear Quadratic Regulator |
| MIMO | Multiple input multiple output |
| MOSFET | Metal-Oxide-Semiconductor Field-Effect Transistor |
| PI | Proportional Integral |
| PID | Proportional Integral Derivative |
| PSO | Particle swarm Optimization |

| | |
|---|---|
| PWM | Pulse Width Modulation |
| SISO | Single input single output |
| VSI | Voltage Source Inverter |

# Chapter 1

# Introduction

## 1.1 Background of Study

The BLDC motors are among the types of motors that are gaining popularity in recent years because the stator of the brushless DC motor is stacked with steel and the windings of the motor are wrapped over the slots. The rotor side is made of permanent magnets. The number of permanent magnets changes between 2 up to 8 pole pairs with north and south poles. In an alternating order, the stator windings should be energized in sequential order to operate the BLDC motor properly..

The synchronous motor is the same as a brushless DC motor with the relationship between current, torque, and voltage. It looks just like a DC motor from a modeling approach. Furthermore, the BLDC motor, the electromagnets, and armature are stationary and the permanent magnets spin. This solves the issue of transferring current to a moving armature. To do this, the brush system commutator component is replaced with a sophisticated electronic controller that distributes power similar to a brushed DC motor [1]. Brushless DC motors have a lot of benefits over brush DC and induction motors, including improved torque-speed characteristics, high dynamic response, high efficiency, reliability, long operating life, noiseless operation, and a wide speed range. The supplied torque to motor size ratio is higher making it useful in application areas - such as aerospace, a wide range of applications, robotics, industrial process control, automotive electronics, and household appliances[2],[3],[4].

In the BLDC motor, power transistors are used for changing the polarity which is performed by switching the transistors in synchronization with the rotor position. The BLDC motors often include hall sensors to sense the actual rotor position and brushless DC Motors are

utilized in a range of industrial applications, such as traction drive and electric vehicles. Electric vehicles (EVs) are vehicles with electric propulsion systems that are either partially (Hybrid Electric Vehicles, HEVs) or (Battery Electric Vehicles). BLDC motors provide traction features such as a high starting torque and a high efficiency of 95 to 98 % then BLDC motor is used for traction purposes. A BLDC motors are suitable for a high power density design approach.
The BLDC motors are the most preferred motors for electric vehicle application due to their traction characteristics so that the BLDC motors are used in many different power ratings from very small motors ratings as used in hard disk drives to large motors in electric vehicles. Most application areas are used to three-phase motors but two-phase motors are also found. The BLDC motors have many advantages over brushed DC motors.A few of them are:

- higher speed ranges.
- higher efficiency.
- better torque speed characteristics.
- long operating life .
- noiseless operation .
- higher dynamic response.

One of the most fundamental optimum control issues is the linear quadratic Gaussian(LQG). It is about additive white Gaussian noise driving linear systems. The goal is to find an output feedback law that minimizes the predicted value of quadratic cost criteria while remaining optimal. The beginning state is also considered to be a Gaussian random vector and output measurements are supposed to be contaminated by Gaussian noise. The uncertainty factors due to parameter changes of motor resistance, inductance, and a load of the system must be translated into a weights matrix based on the state-space model. The performance criteria exist for the selection of weighting matrices and also they are specific to the system. Usually, suitable weights of LQG control are obtained by the trial and error method. But to use the particle swarm optimization techniques to adjust the gain parameter of the LQG controller based on the BLDC motor state space, and to achieve the performance for reference tracking and against disturbances, uncertainties, and noise, a control strategy that relies on Linear-Quadratic Gaussian (LQG) controllers is tuned with the weighting matrices are optimized by PSO, and the LQG controller requires the state-space modeling, thus the modeling of the brushless represent in the state-space model[5].

In this thesis, the electric vehicle dynamics mathematical modeling is performed. Also, the mathematical model and the principle of a three-phase star-connected BLDC motor drive with an ideal trapezoidal back-EMF waveform are discussed. The comparison of PI and PSO-LQG speed controllers for BLDC motor control is performed. The result shows PSO-LQG speed controller gives better speed performance than the others. Besides the motor is controlled in all four quadrants without any loss of power; in fact, energy is conserved during the braking period. The brushless DC motor model is designed and simulated using MATLAB/SIMULINK.

## 1.2 Statement of Problem

The environment is influenced by a variety of factor which is one of the world's major issues Vehicles with internal combustion engines generate carbon dioxide into the environment this factor produce Cars using internal combustion engines. Then to fix this problem it is essentially replacing internal combustion engine autos with electric vehicles into account the aforementioned issues. When replacing an ICE with an electric motor, however, consideration should be given to vehicle speed, weight, cost, comfort, reliability, and compactness.
This paper presents a PSO-LQG-based speed control of a brushless DC motor(BLDC). The brushless DC motor has the following special features for EV because the motor has higher speed ranges, better speed versus torque characteristics, long operating life, higher efficiency, and high start torque. This advantage makes the BLDC motor becomes popular in the EV application, but this motor is a non-linear system. The suggestion of the PSO-LQG controller is to minimize nonlinearities and uncertainties caused by BLDC motor reference input variations, guaranteeing a fast and accurate dynamic response with excellent steady-state performance. If the EV is planned to operate in a variety of driving cycles, such as urban and highway driving cycles, the motor was chosen must be developed and managed to provide better electromagnetic performance in each drive cycle and higher starting electromagnetic performance necessitates a vehicle with a maximum torque output for acceleration.

## 1.3 Objectives of The Study

### 1.3.1 General Objective

The main objective of this thesis is to design and simulate an LQG Controller tuned with PSO for speed control of the brushless DC motor drive and to analysis the performance for the purpose of EV application.

### 1.3.2 Specific Objectives

- To model the BLDC motor.
- To design LQG Controller and PI controller for BLDC motor.
- To simulate the controller and tune using PSO.
- To evaluate the performance of the speed control of BLDC motor.

## 1.4 Scope and Relevance

This thesis included the specification of model generation and analysis of speed control of the BLDC motor using the PSO-LQG controller. Specifically, the three-phase voltage, current, torque, and speed were computed using mathematical modeling of BLDC motor and used for extraction of machine parameters such as coil inductance, Rotor inertia, damping constant, and resistance to compute motor performance characteristics like torque, rotor speed, phase current, hall sensor, and back emf is performed. After the model is built and its characteristics are analyzed, a controller configuration that will be more appropriate for EV application is suggested. In this thesis, the effectiveness and efficiency of the LQG controller tuned with PSO-based brushless motor will be illustrated theoretically as well as mathematically and it will be compared to using conventional PI controller strategy. The theoretical explanation will be validated using a computer simulation and to make the simulation is done by MATLAB/ SIMULINK will be employed.

## 1.5 Motivation

As the global economy moves towards clean energy in the face of climate change the automotive industry is researching on improving the performance of automobiles. electric vehicles (EVs) are the answer to the imminent crisis. But the question that is always asked is how can the driving limit for electric vehicles be increased. The answer to this question lies in the success of investigations. The development of electric machines requires a market at a competitive price. The motor studied in this thesis is a machine that has its power rate, torque control, and speed control.

## 1.6 Methodology

The following methods will be used to complete the research:

- Literature Survey:Start by studying the literature, which includes reading books, journal articles, and thesis works to gather important information, concepts, and ideas that will help you focus on the thesis.
- System modeling :Formulating mathematical model based on the dynamics of the BLDC motor
- Controller design:Design the proposed controllers based on the formulated mathematical model
- Analysis and interpretation:Simulation result analysis and Discussion
- MATLAB/Simulink Simulation has been utilized for comparison Compare PSO-LQG with PI

## 1.7 Thesis Organization

The thesis is organized into six chapters including this introduction.The rest of the thesis is organized as follows.
**Chapter 2** introduction about the brushlees dc motor.A short summery for the reviewed articles is included in the literature review section of this chapter.

**Chapter 3** describes the theory and operation principles of BLDC. Dynamical modeling of BLDC with hysterics current (reference current generator) also described.

**Chapter 4** in this chapter the concept behind the proposed LQG controller, PI controller,LQR controller ,and LQE controller are tried to be covered.

**Chapter 5** shows and discusses the simulation results of the drive system on MATLAB/SIMULINK .The results section focuses on the performance of no-load speed controller, loaded speed controller and at the end of the result section the LQG tuned with PSO control performance is tried to be compared with the PI control.

**Chapter 6** write the conclusion from the developed simulation in this thesis and recommend further research possible in this area.

# Chapter 2

# Theoretical Background and Literature Review

## 2.1 Introduction

The theoretical explanation of the BLDC motor, as well as a literature review and related work for BLDC motor speed control, are discussed in this chapter. The first section discusses brushless dc motor construction, working principle, advantages, Disadvantages, and Applications.
The second section literature review shows the variation of the mathematical modeling, controller designs, and optimization techniques for BLDC and the EV application system which are incorporated with the motors for further investigation. In the final section related to work in the research is discussed.

## 2.2 Construction,Working Principle and Applications of BLDC (Brushless DC Motor)

Brushless DC motors(BLDC)have been a wide topic among motor manufacturers, since they are becoming the preferred choice in a growing number of applications, particularly in the field of motor control technology. In many aspects, the BLDC motors outperform brushed DC motors including the ability to run at high speeds, high efficiency, and better heat dissipation. It is an essential component of the application of modern drive technology including electric propulsion, robotics, computer peripherals, and electrical power generation. A brushless DC motor(also known as BLDC)is a permanent magnet synchronous electric motor that

is powered supplied by direct current(DC) electricity and uses an electronically controlled commutation system rather than a mechanically controlled commutation system to produce rotational torque in the motor. Trapezoidal permanent magnet motors are another name for BLDC motors.

### 2.2.1 Construction of BLDC Motor

BLDC motors are available in a variety of physical configurations. Depending on the stator windings these motors can be configured as single-phase, two-phase, and three-phase. The construction of this motor is similar to that of a three-phase induction motor or a normal DC motor. The stator of a BLDC motor is made up of stacked steel lamination to carry the windings. These windings are inserted into slots in the stator's inner periphery which are cut axially. A star or a delta pattern can be used to organize the windings. Most BLDC motors have a three-phase star-connected stator. The rotor of a BLDC motor contains a permanent magnet. The number of poles in the rotor can range from 2 to 8 pole pairs with alternate south and north poles depending on the application and to achieve maximum torque in the motor the flux density of the material should be high. The rotor must be composed of the right magnetic material to achieve the required magnetic field density[6].

### 2.2.2 Working Principle of BLDC Motor

Brushless DC motors operate similarly to standard DC motors. As a result of the reaction force, the permanent magnet will experience an equal and opposite force. The current-carrying wire will remain stationary in a BLDC motor while the permanent magnet moves. When an electrical supply source switches the stator coils it converts into an electromagnet producing a consistent field in the air gap. The switching results in the back emf voltage waveform with a trapezoidal shape are generated. So that the force of interaction between the electromagnet stator and the permanent magnet rotor continues to rotate.

### 2.2.3 Advantages,Disadvantages and Applications of BLDC motor

**Advantages of Brushless DC Motors**

BLDC motors have several advantages over traditional DC motors,including the following:

- Better speed versus torque characteristics.
- High efficiency due to the use of permanent magnet rotor.
- Smaller motor geometry and lighter in weight than both brushed type DC and induction AC motors.
- Long-life as no inspection and maintenance is required for commutator system.
- High speed of operation even in loaded and unloaded conditions due to the absence of brushes that limits the speed.
- Long operating life due to a lack of electrical and friction losses.
- Noiseless operation.

**Disadvantages of Brushless DC Motor**

- These motors are costly
- The electronic controller required to control this motor is expensive
- Not much availability of many integrated electronic control solutions, especially for tiny BLDC motors

**Applications of Brushless DC Motors**

Brushless DC Motors are utilized for a wide range of applications in the sectors of industrial control, automotive, aviation, automation systems, health care equipment, and so on. They can handle variable loads, constant loads, and positioning.

Some specific applications of BLDC motors are:

- Electric vehicles,hybrid vehicles,and electric bicycles
- Industrial robots,CNC machine tools,and simple belt-driven systems
- Washing machines,compressors,and dryers e.t.c

## 2.3 Electric Vehicles

Electric vehicles are becoming more popular because they not only reduce noise and pollution but can also be used to lessen transportation reliance on oil as long as the electricity is supplied using non-oil fuels. Electric vehicles can also help to cut down on greenhouse gas emissions. Electric vehicles must be powered by non-fossil fuel sources such as nuclear and alternative energy to produce zero carbon dioxide emissions. A hybrid vehicle has two or more power sources allowing for a wide range of options. The most common hybrid vehicles combine an internal combustion engine (IC engine) with a battery, as well as an electric motor and generator[7].

Electric vehicles are not new to the modern world, but their inventive advancement and greater concern about pollution control have earned them the label of future mobility. Electric energy is the most common source of power for vehicle drive in EVs. Electric motors convert electrical energy into mechanical (rotational) energy in electric vehicles through a proper transmission system. This rotational energy is transmitted to the wheels of a vehicle. In the world of electric vehicles, a vehicle with four wheels can be regarded as the most efficient vehicle [8]. Electric vehicles can either run entirely on electricity or use batteries in conjunction with gasoline engines to control the vehicle. Any electric vehicle's essential components are the battery, electric motor, and controller.

## 2.4 Literature Review

**Introduction**

The following literature shows the variation of the mathematical modeling, controller designs, and optimization techniques for BLDC and the EV application system which are incorporated with the motors for further investigation.

In the work given by [9], the author discussed a new optimal PI/PID controller tuning algorithm is proposed for the low-order delay process through the LQR method. The closed-loop system requires the natural frequency and damping ratio, hence a novel criterion for selecting the Q and R matrices is proposed. Various dynamic examples are presented to demonstrate the effectiveness of the adjustment algorithm and show a significant improvement over the existing PID adjustment approach. But the drawback of this paper doesn't consider the disturbance.

The authors of[10], propose that a particle swarm optimization method determines the optimal proportional integral derivative(PID)controller parameters for the speed control of

linear brushless DC motors. This method has the advantages of simple implementation, stable convergence characteristics, and high computational efficiency. The brushless DC motor is modeled in the Simulink model and the PSO algorithm is implemented in MATLAB. The performance analysis is to compare with the genetic algorithm (GA) and the linear quadratic regulator(LQR)method. The LQR method is more effective in improving the step response characteristics, such as reducing the steady-state error, the rise time, settling time, and maximum of linear brushless DC motors Over speed control.

The authors propose a novel PID control design that is both efficient and effective. The linear quadratic regulator approach is used to find the best parameters for the PID controller. The output signal is the sole thing that the improved state vector for performance measurement pertains to Pole assignment determines the weighting function. The best PID controller existence criterion is derived. The BLDC motor speed is controlled using the new PID tuning method. The performance of the optimal LQR controller is better than that of the typical PID controller, according to computer simulation and experimental results [11].

The work given by [12], discussed the implementation of Linear Quadratic Gaussian(LQG)and Extended Kalman Filter(EKF)for DC motor position control.LQG is a widely used linear optimal control technology. However, the direct implementation of LQG using the Kalman filter as the best estimator cannot adapt to changes in system parameters resulting in deviations from the expected best performance.EKF allows the estimation of system parameter values and the unknown state of the system. The estimated value is used to continuously update the plant model and to calculate the gain for optimal performance. The limitation of this work is that the gain parameters are adjustment using by manually there is no tuning technique is used.

The author explained the Position control of DC motors using the LQR is more robust in comparison to other non-adaptive controllers and adaptive controllers like the PID Controller and the Fuzzy Logic Controller(FLC) respectively[13].LQR has been used to improve the PID model for speed control as well as other adaptive controllers such as feedback linearization. The weight matrix of the LQR controller must be manually adjusted, which is a limitation of this research.

The authors propose that a three-phase star-connected brushless DC motor model considering the behavior of the motor during commutation. This process was completed in MATLAB/SIMULINK after the BLDC motor with sinusoidal and trapezoidal back-EMF waveforms was developed. Comparative study between MATLAB/SIMULINK models The sinusoidal and trapezoidal models of back EMF[14]. The limitation of this work there not consider the position sensor and speed, it is dealing with the compression of the commutation system. In the work given by [15], the authors explained the speed control of an

optimized controller based on PSO is implemented and the Brushless DC motors are introduced. Now,the BLDC motors are widely used in many industrial and vehicle applications, due to their long service life, high dynamic response, high efficiency, and better torque-speed characteristics. This work demonstrates the use of MATLAB/SIMULINK to build a brushless DC motor model to evaluate the performance of a BLDC motor controller with a PID-PSO control scheme. The presented model shows that the speed is regulated by a PID controller optimized by PSO technology. In motor-driven variable speed applications. The use of BLDC motors has been widely used, because the BLDC motors have a higher speed range, higher torque-to-weight ratio, and simpler structure, and also have better torque-speed characteristics and better dynamic response. Then the limitation of this work is there is no consider disturbance band rejection. The authors state the mathematical model to perform a novel modeling and simulation approach for brushless DC motor control systems. In the MATLAB/SIMULINK environment the brushless DC motor model, the voltage type inverter circuit model, the hysteresis current tracking comparative model, and the PID speed controller model were built [16].

The authors focus on Electric vehicles are transportation trendsetters since they emit no greenhouse gases and they are more efficient. Brushless DC motors are the most common type of motor utilized in electric vehicle applications. For effective speed control of the BLDC motor, a Hybrid Fuzzy PI controller is used. The Fuzzy logic controllers(FLC)optimize transient performance and reduce steady-state inaccuracy in general. The PI speed controller performs well in the steady-state but not so well in the transient. The referenced Hybrid fuzzy PI controller combines the advantages of the two controllers to achieve good performance.In addition, this research compares the $PI, FLC$, and Hybrid Fuzzy PI controllers for a BLDC motor[17].The BLDC motor with the controller is designed and simulated in the MATLAB/SIMULINK environment. The results demonstrate the superiority of the proposed Hybrid Fuzzy PI for BLDC motors. In the work given by [18], explain the Different electric motors are investigated and compared in this study to determine the benefits of each motor and which one is best suited for usage in electric vehicle(EV)applications motor like DC motor, induction motor, permanent magnet synchronous, switching reluctance, and brushless DC motors are analyzed. The conclusion is that, while induction motor technology is more advanced than others, but brushless DC and permanent magnet motors are better suited for EV applications. These motors will produce less pollution, consume less fuel, and have a higher power to volume ratio. Permanent magnet materials are becoming more affordable. Permanent magnet and brushless DC motors are becoming more efficient making them more appealing for EV applications.

According to the above literature review, most researchers have focused on the design of

the BLDC motor using PI, PID, Fuzzy, and LQR controller there no consider the effect of disturbance and the parameter variation. for example, the author Gwo-Ruelyyu and Rey-the state that the speed control of BLDC motor using PID controller and LQR approach, from this result the gain parameter of PID controller is adjusted by trial and error there is no use the optimization techniques, and the weighting function of the LQR controller parameter selected by using pole placement. So the problem of this paper does not consider the effect of the disturbance on the system and the gain parameter adjusted by trial and error. To fix the problem of above problem to use the LQG- PSO controller, where the LQG controller parameters are tuned online according to the error and change of error. The LQG -PSO control optimization technique is used to Adjust the values of the gain. .

## 2.5 Related Works

### 2.5.1 Literature Review of Research in Modeling of BLDC Motor

The motor mathematical modeling, the back emf waveform, rotor position(hall sensor), and the speed control of BLDC motor using PI of this thesis is directly related to a novel study made by [19], to deal with a wide range of applications. In comparison to a DC motor, the BLDC motor has an electronic commutator that replaces the mechanical commutator to make it more reliable. Rotor magnets generate the magnetic flux in BLDC motors to allowing them to attain higher efficiency. By using a hall sensor the commutation ensures that the BLDC motor's rotor rotates properly, while the motor speed is determined by the magnitude of the supplied voltage. The PWM technique is used to change the value of the applied voltage. A speed controller, which is implemented as a traditional (PI)controller. The difference between the actual and necessary speeds is fed into the PI controller, which subsequently adjusts the duty cycle of the PWM pulses that correspond to the required voltage amplitude to maintain the desired speed.

### 2.5.2 Brushless DC motor control Using Hybrid Technique

#### Proportional Integral Controller -Particle Swarm Optimization

The design of the BLDC motor drive is a complex process that includes modeling, control scheme selection, and parameter tuning among other things. This work is being studied to obtain a better understanding of the system and to tune the controller parameters of the control system to achieve the best possible performance. Various new control systems for the

speed control design of BLDC motors have recently been developed[15]. This work presents the model construction of a brushless DC motor with MATLAB/SIMULINK to evaluate the performance of the BLDC motor control with a PID -PSO Controller scheme. The model presented to display the speed is regulated by PID Controller optimized by the PSO technique. In variable speed application of motor drives utilization of BLDC motor has been widely used because the BLDC motors have Higher Speed Range, Higher Torque vs Weight Ration, and simpler structure. They have improved speed to torque characteristics as well as greater dynamic responsiveness. In fact most industrial processes with different degrees of nonlinear, parameter variability, and uncertainty of mathematical model of the system. The tuning PID control parameters are very poor robustness. Therefore, it's difficult to achieve the optimal state under field conditions in the actual production.

### 2.5.3 Modeling of LQG controller and tune with PSO

The state-space representation, the gain adjustment of the parameter, mathematical modeling, and the speed control of BLDC motor using LQR of this thesis is directly related to a novel study made by[20]. This paper is done regulating and tracking the speed of the motor at desired speed is an important application in automotive industries. So we use an LQR controller to regulate the speed and position of the motor, to measure the state feedback gain, identify state variables, and control variables of the BLDC drive system are done in this thesis. The main objective of this paper is to formulate the control law which results in a minimum performance index, to adjust the gain parameter, and to check the performance of the plant. But the drawback of this paper is there is no estimate of the state variable and the automatic gain adjustment.

The authors in,[21]address the application of soft computing algorithm design based on linear quadratic Gaussian(LQG)controller parameters optimization through the genetic algorithms has been applied to control the speed of the DC motor. The Optimum LQG Controller, which is consists of the feedback gain (K)and the Kalman filter gain(L)is an optimal control method that could efficiently achieve the tacking performance. This increases the robustness of the system and gives better performance. The result obtained show that the selected approach used in the choice of matrix Q, R, W, and V achieves very good performance. The tuning of the Genetic algorithms to be a part automatic adjustment for the gain parameter of the linear-quadratic Gaussian controller design to be a tremendous offline or online design process.

# Chapter 3

# System Modeling

## 3.1 Introduction

The first section is the mathematical modeling of the proposed motor BLDC including the analysis motor using parameters and variables in the ABC reference. The mathematical modeling covers the motor structure, principles of operation, voltage equations, principle of torque generation, and current limits for this particular motor.

In the second section, the PWM technique for generating pulse signals to the inverter will be discussed. It is obvious that the BLDC motor must be supplied from a well-controlled inverter for a variable speed drive operation. And inverter gate signal generations were discussed briefly.

## 3.2 Brushless DC Motor

### 3.2.1 Introduction of the Motor

A BLDC motor is a permanent magnet synchronous motor. Position sensors are used to sense the rotor position according to the rotor position to control the stator currents and the speed of the motor. The term DC comes in the name of BLDC because its torque-speed characteristics are similar to that of DC motors. The BLDC requires an electronic commutation circuit instead of mechanical or brushed commutation used in DC motor. In the BLDC motors, the back-EMF waveform induced is trapezoidal. The trapezoidal waveform requires a rectangular current to achieve high torque.
The trapezoidal motors need a position sensor to detect the position of the rotor at any

time. It requires complex hardware to run smoothly. The trapezoidal back emf waveform of the motors is more popular in most applications due to their simple operation, low price, and high efficiency. The BLDC motor with star-connected winding configurations generates high efficiency and low speed.

### 3.2.2 The Structure of the Motor

The Structure of the BLDC motor is identical to the AC(asynchronous)and DC motors. A BLDC motors stator is made up of stacked steel laminations with slots on the inner periphery. The stator windings can be connected in two ways namely Star and Delta connections. The value of torque is high and speed is low when the stator windings are connected in a star configuration. Each of these windings is made up of multiple interconnected coils with one or more coils arranged in the stator slots. Because half of the input voltage is supplied across the winding in a delta connection the value torque and speed are low and the coil distribution on the stator periphery the output torque of a sinusoidal motor is smoother than that of a trapezoidal motor. This comes at a cost as sinusoidal motors require more winding interconnections.

The rotor of the BLDC motor is not connected to the supply, and it is made up of permanent magnet steel. The ferrite magnets are utilized to make BLDC rotors because they are less expensive. But they have the drawback of having a low flux density and rare earth alloys such as Neodymium, Samarian cobalt, Neodymium ferrite, and Boron are now utilized in technology.

The electronic commutator is distinguished from typical commutators to control the BLDC motor. In BLDC motors the Hall Effect Sensors $Ha, Hb$, and $Hc$ are displaced by a $60^o$ phase shift. The electronic commutator energizes the BLDC motor winding enabling the stator to form poles and the permanent magnet rotor is rotated according to the commutation sequence. The rotor position is sensed using hall Sensors. This will make the digital signal high or low allowing the rotor positions to be recognized.

### 3.2.3 Principle of Operation of Brushless DC motor

The three-phase BLDC motor is operated in a two-phase ON mode, which means that the two phases that generate more torque are activated, while the third phase is turned off. The rotor position determines which two phases are energized. The position sensor signals provide a three-digit number that changes every $60^o$(electrical degrees)to control the hall

sensor $Ha, Hb, Hc$ as shown in Figure 3.1.

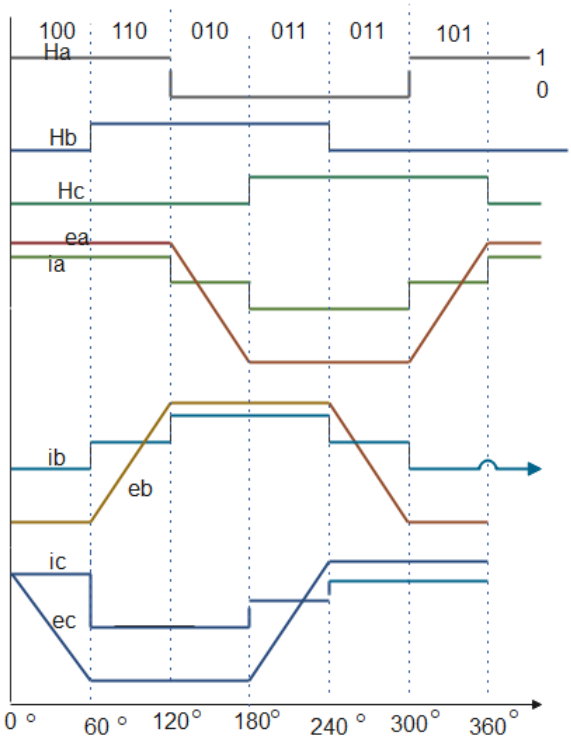


Figure (3.1) Back emf, phase current and rotor position

The waveform of ideal current and reverse emf are also shown in the diagram 3.1 [22].Table 3.1 [23],shows a simplified version of how a six-step inverter handles current commutation. Although bipolar junction transistors are depicted MOSFET switches are the most frequent. The switching sequence, current direction, and position sensor signals are shown in the table 3.1.

Table (3.1) Over all sequence of Hall sensor,Switching sequence and Phase current operation of BLDC motor

| **Switching Interval in Degree** | **Sequence Number** | **Position Sensors** | | | **Switch Closed** | | **Phase Current** | | |
|---|---|---|---|---|---|---|---|---|---|
| | | H1 | H2 | H3 | | | **A** | **B** | **C** |
| 0 – 60 | 0 | 1 | 0 | 0 | S1 | S4 | + | – | Off |
| 60 – 120 | 1 | 1 | 1 | 0 | S1 | S6 | + | Off | – |
| 120 – 180 | 2 | 0 | 1 | 0 | S3 | S6 | Off | + | – |
| 180 – 240 | 3 | 0 | 1 | 1 | S3 | S2 | – | + | Off |
| 240 – 300 | 4 | 0 | 0 | 1 | S5 | S2 | – | Off | + |
| 300 – 360 | 5 | 1 | 0 | 1 | S5 | S4 | Off | – | + |

### 3.2.4 Modeling of Brushless DC Motor

Modeling of a BLDC motor can be developed similarly to a three-phase synchronous machine. There is a permanent magnet mounted on the rotor and some dynamic characteristics are different from a synchronous machine. Flux linkage from the rotor depends upon the magnet material. As a result, this type of motor is prone to magnetic flux saturation. A three-phase voltage supply feeds one structure of the BLDC motor much like any other three-phase motor. It is not necessary for the source to be sinusoidal, Square wave or any other waveform can also be used as long as the peak voltage does not exceed the motor maximum voltage limit. The BLDC motor is a permanent magnet motor with trapezoidal back EMF, whereas the synchronous motor has sinusoidal back EMF. The trapezoidal mutual inductance connection between stator and rotor is non-sinusoidal[3]. So, transforming to the d-q axis does not provide any added benefit, thus phase a phase b, phase c are variable models is chosen. In the present model, the motor is assumed to be star-connected with isolated neutral. The analysis is based on the following assumptions:

- The motor is not saturated and should be operated with the rated current .
- Stator resistances of all the windings are equal.
- Self-inductance and mutual inductance are constant.
- Iron and stray losses are negligible .
- Three phases are balanced.
- Uniform air gap.
- Hysteresis and eddy current losses are not considered.
- Power semiconductor devices in the inverter are ideal.

. The circuit equations of the three windings in phase variables can be found in the [24],[25],[23]. On the rotor side, the BLDC motor has three stator windings and a permanent magnet rotor. Due to the high resistance of both magnets are stainless steel and rotor-induced currents can be ignored. The motor is powered by three-phase voltage sources and the modeled equations in phase variables for three armature windings [24],[25], [26] are as follows.

### 3.2.5 Voltage Equation

In the model of the armature winding for the BLDC motor, the voltage equation is expressed as referring to the circuit in the figure 3.2[27]. The following voltage equations are obtained [23].

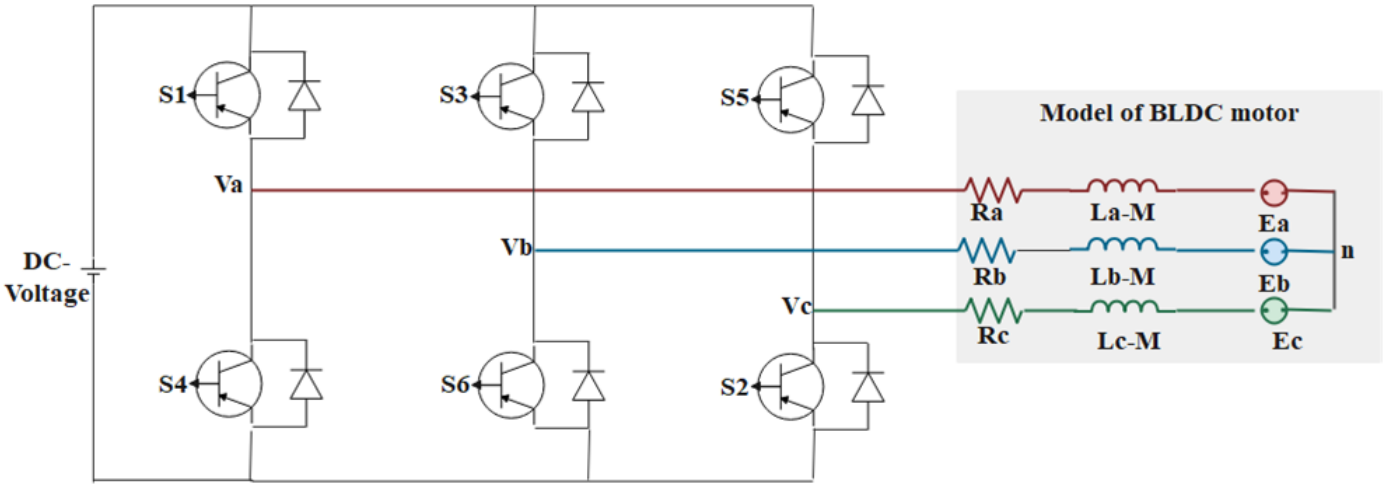


Figure (3.2) Equivalent circuit of brushless DC motor

$$
\begin{aligned}
v_a &= R_a i_a + L_a \frac{di_a}{dt} + M_{ab} \frac{di_b}{dt} + M_{ca} \frac{di_c}{dt} + e_a \\
v_b &= R_b i_b + L_b \frac{di_b}{dt} + M_{ab} \frac{di_a}{dt} + M_{bc} \frac{di_c}{dt} + e_b \\
v_c &= R_c i_c + L_c \frac{di_c}{dt} + M_{ca} \frac{di_a}{dt} + M_{bc} \frac{di_b}{dt} + e_c
\end{aligned} \tag{3.1}
$$

Suppose that the following assumption that the motor is perfectly balanced.The three phases are identical and all parameters are equal i.e $R_a = R_b = R_c = R, L_a = L_b = L_c = L$ ,and $Mab = Mbc = Mca = M$. Where $V_a, V_b$,and $V_c$ are the phase voltage,$i_a, i_b$ ,and $i_c$ are the phase current, $e_a, e_b$ ,and $e_c$ are the phase back EMF,$R_a, R_b$ ,and $R_c$ are the resistance of each phase, $L_a, L_b$ ,and $L_c$ are the self inductance of each phase and $Mab, Mbc$ and $Mca$ are the mutual inductance between two phases .Then to simplify equation 3.1 to get:

$$
\begin{aligned}
v_a &= Ri_a + L \frac{di_a}{dt} + M \frac{di_b}{dt} + M \frac{di_c}{dt} + e_a \\
v_b &= Ri_b + L \frac{di_b}{dt} + M \frac{di_a}{dt} + M \frac{di_c}{dt} + e_b \\
v_c &= Ri_c + L \frac{di_c}{dt} + M \frac{di_a}{dt} + M \frac{di_b}{dt} + e_c
\end{aligned} \tag{3.2}
$$

The stator phase currents are considered to be balanced using Kirchhoff current law.

$$i_a + i_b + i_c = 0 \tag{3.3}$$

Both sides multiply by M for equation 3.3 become :

$$Mi_a + Mi_b + Mi_c = 0 \tag{3.4}$$

Then to rearrange Equation 3.3

$$-Mi_a = Mi_b + Mi_c \tag{3.5}$$

To substitute equation 3.5 in to equation 3.2 which gives.

$$\begin{aligned} v_a &= Ri_a + L\frac{di_a}{dt} - M\frac{di_a}{dt} + e_a \\ v_b &= Ri_b + L\frac{di_b}{dt} - M\frac{di_b}{dt} + e_b \\ v_c &= Ri_c + L\frac{di_c}{dt} - M\frac{di_c}{dt} + e_c \end{aligned} \tag{3.6}$$

The per phase terminal voltage in terms of the motor armature parameters and back emf motor Voltage is express by:

$$\begin{aligned} v_a &= Ri_a + (L - M)\frac{di_a}{dt} + e_a \\ v_b &= Ri_b + (L - M)\frac{di_b}{dt} + e_b \\ v_c &= Ri_c + (L - M)\frac{di_c}{dt} + e_c \end{aligned} \tag{3.7}$$

Then to from above equation 3.7 the value of M is very small from this L-M=L the voltage equation become,[3].

$$\begin{aligned} v_a &= R_a i_a + L\frac{di_a}{dt} + e_a \\ v_b &= R_b i_b + L\frac{di_b}{dt} + e_b \\ v_c &= R_c i_c + L\frac{di_c}{dt} + e_c \end{aligned} \tag{3.8}$$

Rearranging Equations 3.8 gives the three phases of current differential equations as follows

$$\begin{aligned}\frac{di_a}{dt} &= \frac{v_a}{L} - \frac{Ri_a}{L} - \frac{e_a}{L} \\ \frac{di_b}{dt} &= \frac{v_b}{L} - \frac{Ri_b}{L} - \frac{e_b}{L} \\ \frac{di_c}{dt} &= \frac{v_c}{L} - \frac{Ri_c}{L} - \frac{e_c}{L}\end{aligned} \tag{3.9}$$

### 3.2.6 Modeling of Ideal Back-EMF

When the BLDC motor rotates, each winding generates a voltage known as Back EMF. Which is according to Lenz law the opposes the main voltage supplied to the winding the Back EMF polarity is the polarity of the source voltage in the opposite direction and it is related to the function of rotor position. The phase difference between each phase by $120^o$. The Back EMF of the BLDC motor depends on three factors

- The angular velocity of the rotor .
- The magnetic field generated by the rotor magnets.
- The connection in the stator windings.

The back-EMF and the motor current are drawn along with the rotor position sensor signals as shown in Figure 3.3. The induced EMF does not have sharp corners. The back emf wave of the BLDC motor is trapezoidal.

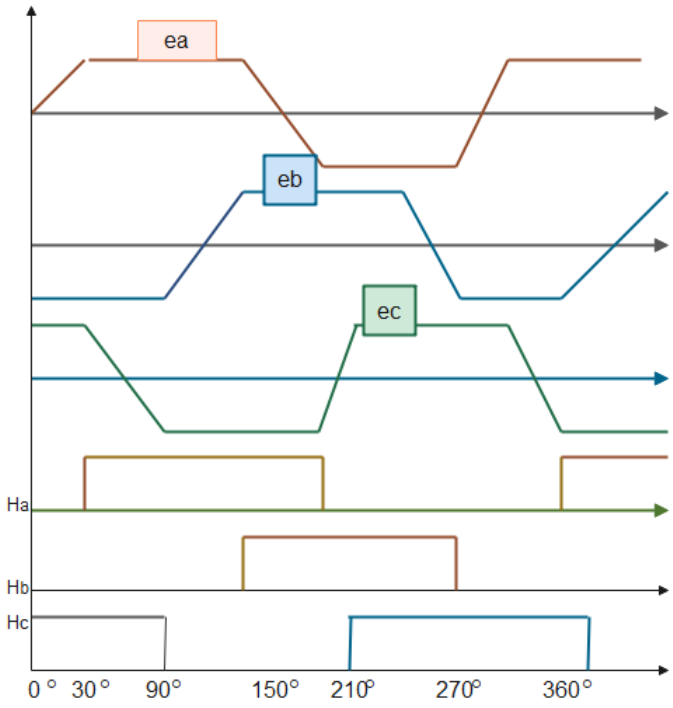


Figure (3.3) Trapezoidal back EMF and phase current variation with rotor electrical angle

From figure 3.3 show that the back-EMF of BLDC motor $e_a, e_b$ ,and $e_c$ have trapezoidal wave.The three-phase back emf of BLDC motor can be described by the following equations,[27].

$$\begin{aligned} e_a &= f_a(\theta_r)\lambda_m\omega_m \\ e_a &= f_b(\theta_r)\lambda_m\omega_m \\ e_a &= f_c(\theta_r)\lambda_m\omega_m \end{aligned} \tag{3.10}$$

or

$$\begin{aligned} e_a &= K_b f(\theta_r)\omega_m = K_b f_a(\theta_r)\omega_m \\ e_b &= K_b f(\theta_r - 120^o)\omega_m = K_b f_b(\theta_r)\omega_m \\ e_c &= K_b f(\theta_r + 120^o)\omega_m = K_b f_c(\theta_r)\omega_m \end{aligned} \tag{3.11}$$

Where $e_a, e_b$ ,and $e_c$ are the induced Back EMF of the motor,$\lambda_m$ is the flux linkage,$\theta_r$ is the electrical rotor angle ,and $\omega_m$ is the mechanical speed of the rotor.The rotor angle functions $f_a(\theta_r).f_b(\theta_r)$ ,and $f_c(\theta_r)$ have the same shape as the back emf of $e_a, e_b$,and $e_c$ with a maximum magnitude of $\pm 1$.As shown below table 3.2[19], that the mathematical functions of the rotor angle in a three-phase system.

Table (3.2) Back-emfs modeled as a normalized function of rotor position

| Rotor position ($\theta_r$) | $f_a(\theta_r)$ | $f_b(\theta_r)$ | $f_a(\theta_r)$ |
|---|---|---|---|
| $0^o - 60^o$ | 1 | --1 | $1 - {}^{6\theta_r}/_{\pi}$ |
| $60^o - 120^o$ | 1 | ${}^{6\theta_r}/_{\pi} - 3$ | $-1$ |
| $120^o - 180^o$ | $5 - {}^{6\theta_r}/_{\pi}$ | 1 | $-1$ |
| $180^o - 240^o$ | -1 | 1 | ${}^{6\theta_r}/_{\pi} - 7$ |
| $240^o - 300^o$ | $-1$ | $9 - {}^{6\theta_r}/_{\pi}$ | 1 |
| $300^o - 360^o$ | ${}^{6\theta_r}/_{\pi} - 11$ | -1 | 1 |

### 3.2.7 Dynamics Modeling of BLDC Motor

The electromagnetic torque for the three-phase BLDC motor is defined as,[19].

$$T_e = \frac{i_a e_a + i_b e_b + i_c e_c}{\omega_m} \tag{3.12}$$

The mathematical model electromagnetic torque can be representing by:

$$T_e = J\frac{d\omega_m}{dt} + B\omega_m + T_L \tag{3.13}$$

Where $J$ is the rotor inertia,$B$ is damping constant,and $TL$ is load torque.

## 3.3 Hysteresis Current Controller

The Hysteresis current controller helps in the formation of the inverter switching signals within the hysteresis band. Hysteresis band PWM is an instantaneous feedback current control method of PWM in which the actual current($i_a, i_b$, and $i_c$) continuously tracks the command current. The working principle of hysteresis band PWM for the inverter is shown in Fig3.4.The control circuit generates the reference current($ia_{ref}, ib_{ref}$,and $ic_{ref}$).It is compared with actual phase current wave ,[28].

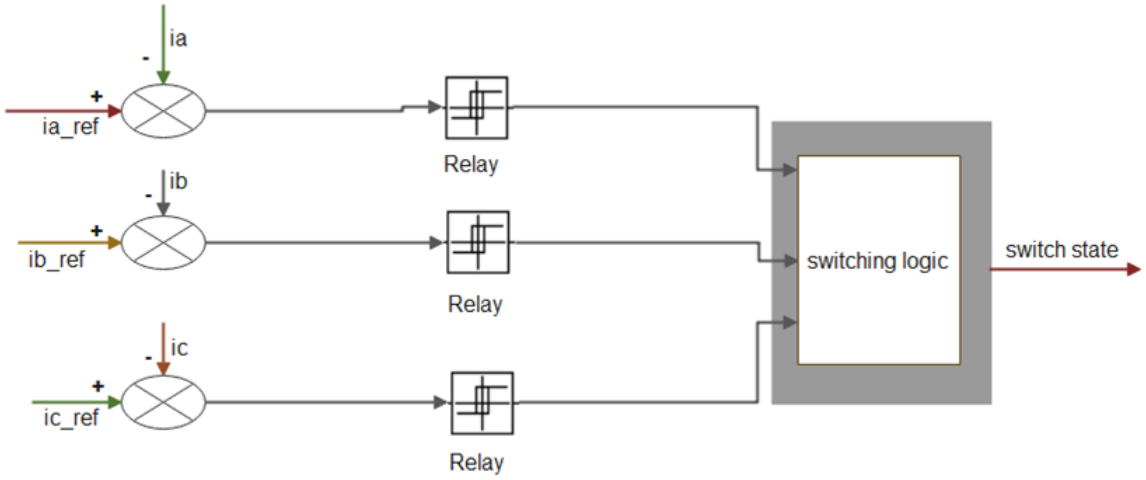


Figure (3.4) The structure of PWM current controller

The upper switch is turned off and the lower switch is turned on when the current exceeds the upper band limit. When the current exceeds the lower band limit the upper switch turns on and the lower switch turns off similar to how the other phase is controlled.

**Reference Current Generator**

The reference current generator is determine by three phase reference phase currents $i_a^*, i_b^*$ ,and $i_c^*$ of the BLDC motor regard to the magnitude of reference current $(i_{ref})$ .Then to calculate the magnitude of reference current $(i_{ref})$ based on the hall sensor(rotor position) $(\theta_r)$ is.

$$i_{ref} = \frac{T_{ref}}{k_t} \tag{3.14}$$

Where $T_{ref}$ is the control signal and $K_t$ is the torque constant for BLDC motor.

Table (3.3) Rotor position signal and Reference currents

| Rotor position $(\theta_r)$ | $i_a^*$ | $i_b^*$ | $i_c^*$ |
|---|---|---|---|
| $0-60$ deg | $i_{ref}$ | -$i_{ref}$ | 0 |
| $60-120$ deg | $i_{ref}$ | 0 | -$i_{ref}$ |
| $120-180$ deg | 0 | $i_{ref}$ | -$i_ref$ |
| $180-240$ deg | -$i_{ref}$ | $i_{ref}$ | 0 |
| $240-300$ deg | -$i_{ref}$ | 0 | $i_{ref}$ |
| $300-360$ deg | 0 | -$i_{ref}$ | $i_{ref}$ |

## 3.4 Three-Phase VSI PWM inverter

Three-phase VSI is operated at the two modes.

1. $180^o$ mode operation
2. $120^o$ mode operation

This thesis uses a $120^o$ mode operation to regulate the power circuit for a BLDC motor. For a three-phase inverter is produce a six-step bridge is employed with six switches and the two switches for each phase are operated. Each step is described as a shift in the operation time from one MOSFET to the next in the correct order.A six-step inverter would have a $360^o$ cycle and each step would be at $60^o$ intervals.$V_s$ is the three-phase source voltage and the MOSFET switches are $S_1, S_2, S_3, S_4, S_5$ ,and $S_6$. The outcomes $V_a, V_b$ ,and $V_c$ are shown in fig 3.2.Three BLDC motors feed this output terminal and $n$ is the three-phase BLDC neutral terminal. The inverter is power circuit diagram is identical to that shown in fig 3.2. Each transistor the $120^o$ mode VSI conduct for $120^o$ of the cycle. To complete one cycle of the output $AC$ voltage the $120^o$ mode inverter takes six steps each of which is $60^o$ long.$S_1$ conducts for $120^o$ in this inverter, but neither $S_1$ nor $S_4$ conduct for the next $60^o$.Now $S_4$ is turned on at $180^o$ and conducts for $120^o$, i.e from 180 to $300^o$ between the $S_4$ stops conducting at $300^o$ and a $60^o$ delay passes until $S_1$ turns on again at $360^o$.The $S_3$ is turned on at $120^o$ and conducts for $120^o$ before being switched off in the bottom row. The $S_6$ is turned on at $300^o$ and conducted for $120^o$and $S_3$ is turned back on after the $60^o$interval has passed. The firing sequences for the six MOSFET switches are identical to those used in the $180^o$ mode inverter. In this situation, just two switches one from the upper group and one from the lower group are active in each step.

# Chapter 4

# Controller Design

## 4.1 Introduction

This chapter presents the theoretical analysis of two different advanced control techniques that are used to achieve a high-performance BLDC motor drive system. The first technique is the PI where the proper parameters are obtained based on the transfer function technique. And the second technique is the LQG control tune parameter gain adjust by using PSO. The optimization mechanism is done online according to the error and the change of error to achieve the required speed tracking.
The Simulation of tuned LQG Controller with PSO for speed control of brushless DC motor shown in the figure 4.1.

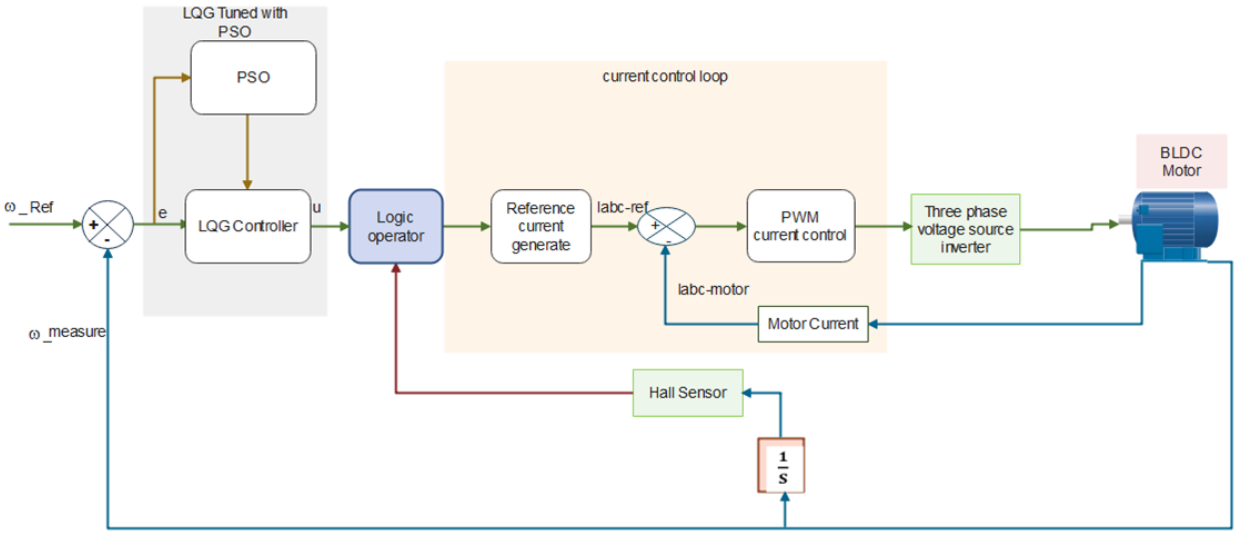


Figure (4.1) General block diagram of LQG Controller tuned with PSO for BLDC

The simulation model of the whole system shown on the block diagram is developed and

simulated on MATLAB/ SIMULINK. In this study is the core simulation containing the control model, motor model, and inverter block. The general block diagram of Figure4.1 shows that phase current and rotor speed are the available feedback. The current command is implemented by the inner current loop, whereas the speed command is implemented by the outer loop. In speed control, the toque command signal is obtained from the speed error signal. The generate the pulse width modulated signal the gate signal is generated for each phase switch by obtaining the phase current error and the error signal with the LQG controller. The LQG gain parameter is adjusted by the PSO algorithm.

## 4.2 Proportional Integral controllers

The goal of the controller is to reduce the error between the actual output that has to be managed and the desired output and also known as the set point. In the instance of speed control the following equation can be used to express the error.

$$e(t) = \omega_{ref} - \omega_{actual} \tag{4.1}$$

Where $e(t)$ is the error function the plant,$\omega_{ref}$is the reference speed or the speed set point ,and $\omega_{actual}$ is the actual motor speed of the motor.
The control signal is proportional to both the error signal and the integral of the error signal in this case. The proportional plus integral controller is mathematically represented as:

$$U(t) = K_p e(t) + K_I \int_0^t e(t)dt \tag{4.2}$$

Where $u(t)$ is the control signal for the output PI Controller,$K_P$ is the proportional gain, and $K_I$ is the integral gain for the PI control. The following block diagram in figure 4.2[29] show that the operation of the speed control using a PI controller and the operation of current control and gate signal generate.

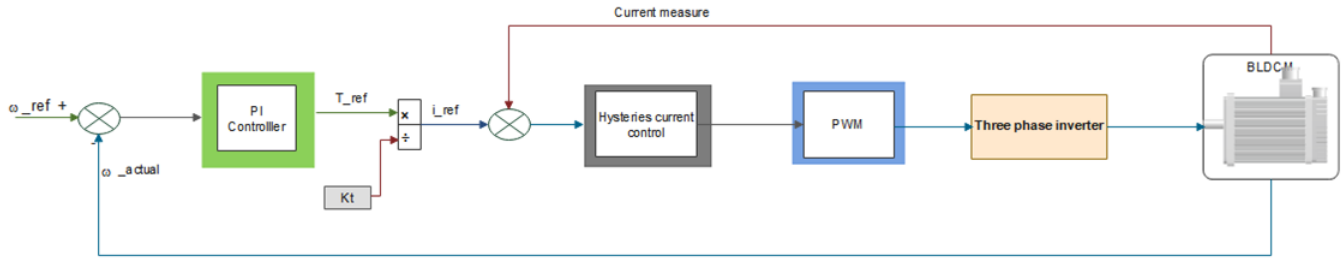


Figure (4.2) Speed control of BLDC motor drive with PI controller

Shows the block diagram representation of the speed control of the BLDC motor drive[30]. The drive scheme consists of an outer and inner current loop for speed and current control respectively. The reference speed and actual speed of the motor are compared to generate the error signal which is given to the PI speed controller for generating the reference current signal. A reference current generator, a PWM current control unit and a three-phase inverter are make up the current control loop. When the actual current signal is compared to the reference current signal to generate an error signal that affects the PWM technique for the duty cycle.

PI controllers are used in the motor drive industry due to their simplicity, robustness, clear functionality, ease to control, and implementation. This controller works well in a linear system and systems with a specified set of known parameters or load conditions. However, when the parameters deviate from the known values the response of the system deteriorates and resulting in poor stability. When the transfer function of the motor drive the system varies with the operating conditions. The controller parameters should adapt to this variation so that the parameters of the PI controller are normally fixed offline and the controller cannot cope with the operating conditions of the drive system.

**Transfer Function Model of the Speed Control Loop BLDC motor**

Transfer functions are usually used to study systems such as SISO and Transfer functions or matrix forMIMO system. Typically within the fields of signal processing, communication theory, and control theory [31]. The term is often used exclusively to refer to linear time-invariant systems. Although most real systems have nonlinear input-output characteristics behavior will be close enough to linear when operated within nominal parameters that linear time-invariant system theory provides an adequate approximation of the input-output behavior. To use from the above equivalent circuit of BLDC motor to calculate the electrical part and the mechanical part for the BLDC motor fig 3.2, and to use equation 3.9 and 3.13 to get:

$$v_a = Ri_a + L\frac{di_a}{dt} + e_a \tag{4.3}$$

And

$$T_e = J\frac{d\omega_m}{dt} + B\omega_m + T_L \tag{4.4}$$

Assume $T_L$ =0 then to calculate the value of current for equation 4.4 become:

$$k_t i_a = J\frac{d\omega_m}{dt} + B\omega_m \tag{4.5}$$

where $T_e = i_a k_t$ then armature current is

$$i_a = \frac{J}{K_t}\frac{d\omega_m}{dt} + \frac{B}{K_t}\omega_m \tag{4.6}$$

To substituting equation 4.6 into 4.3 to get the transfer function of the out put $\omega_m$ with respect to in put $v_a$ is

$$\frac{\omega_m}{va} = \frac{k_t}{L_a J s^2 + (R_a J + L_a B)s + (R_a B + K_t K_b)} \tag{4.7}$$

$$\frac{\omega_m}{va} = \frac{\frac{k_t}{L_a J}}{s^2 + \frac{(R_a J + L_a B)s}{L_a J} + \frac{(R_a B + K_t K_b)}{L_a J}} \tag{4.8}$$

The structure of BLDC motor transfer function with load can be built as shown in Figure 4.3.

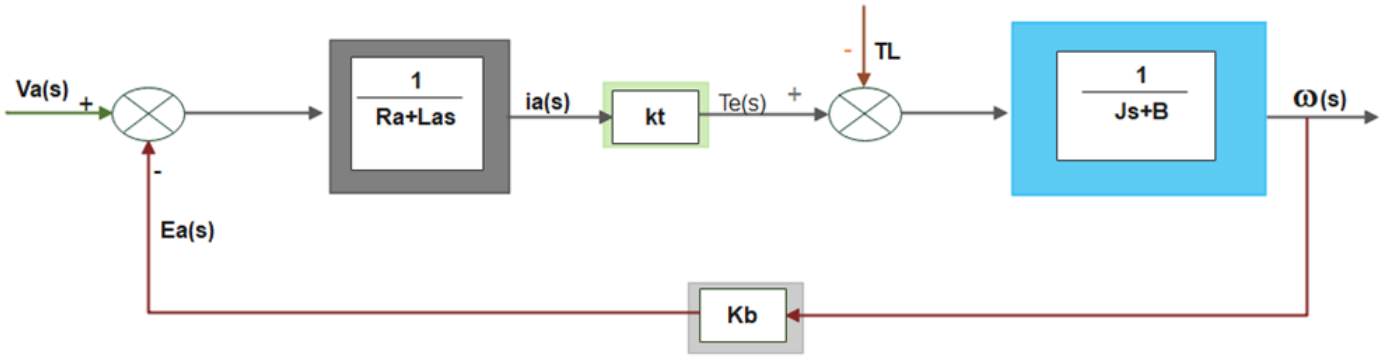


Figure (4.3) Block diagram of the linearized BLDC motor model

Equation 4.9 represents a general second-order system which can be written in the form.

$$G_{OL}(s) = \frac{\omega_n^2}{s^2 + 2\xi\omega_n s + \omega_n^2} \tag{4.9}$$

Where $\omega_n$ is the natural frequency and $\xi$ is the damping ratio of the closed-loop system transfer function. Thus,once the $\omega_n$ and $\xi$ are chosen based on the desired transient peformance requirements,the PI controller parameters can be obtained using the transfer function method the value are $K_P = 5$, $K_I = 2.8$.

## 4.3 Linear Quadratic Gaussian Controller Strategy

### 4.3.1 Introduction

The linear quadratic Gaussian(LQG)controller issue is one of the most fundamental optimal control problems in control theory. It involves a linear system that is driven by additive Gaussian noise. The goal is to find the best output feedback law in terms of minimizing the quadratic cost criterion parameter estimates. The output measurement is affected by Gaussian noise. Optimal control theory involves operating dynamic systems at the lowest cost. The *LQ* problem is defined as the case where the cost is described by a quadratic function and the system dynamics are characterized by a set of linear differential equations. The solution is provided by a linear quadratic regulator (LQR), which is a feedback controller, according to one of the fundamental conclusions of this theory. Solving LQG problems requires the use of LQR. The LQG problem is one of the most fundamental problems in control theory, much like the LQR problem.

Linear Quadratic Gaussian control is an optimal control. It is a combination of LQR (linear quadratic regulator)and Kalman filter [32]. This is very useful because not all states of the system can be measured. Replacing the sensor with an observer also reduces the cost of the system. However, it cannot guarantee the robustness of the system under uncertainty in operating conditions. The Kalman filter is used to estimate the state of the system based on the output of the system. The estimated state is sent to the LQR control as state feedback. The Kalman filter needs a system model to estimate the state of the system. Therefore, a system model is needed. The system model is constructed based on mathematical equations or based on input and output modeling system data. The design of the LQG control system is carried out in two steps. First, to design a linear quadratic regulator and a linear quadratic estimator(LQE or Kalman filter). Finally to integrate the two systems into a single control structure usually called the LQG controller. Then LQG control block diagram is shown in Figure 4.4.

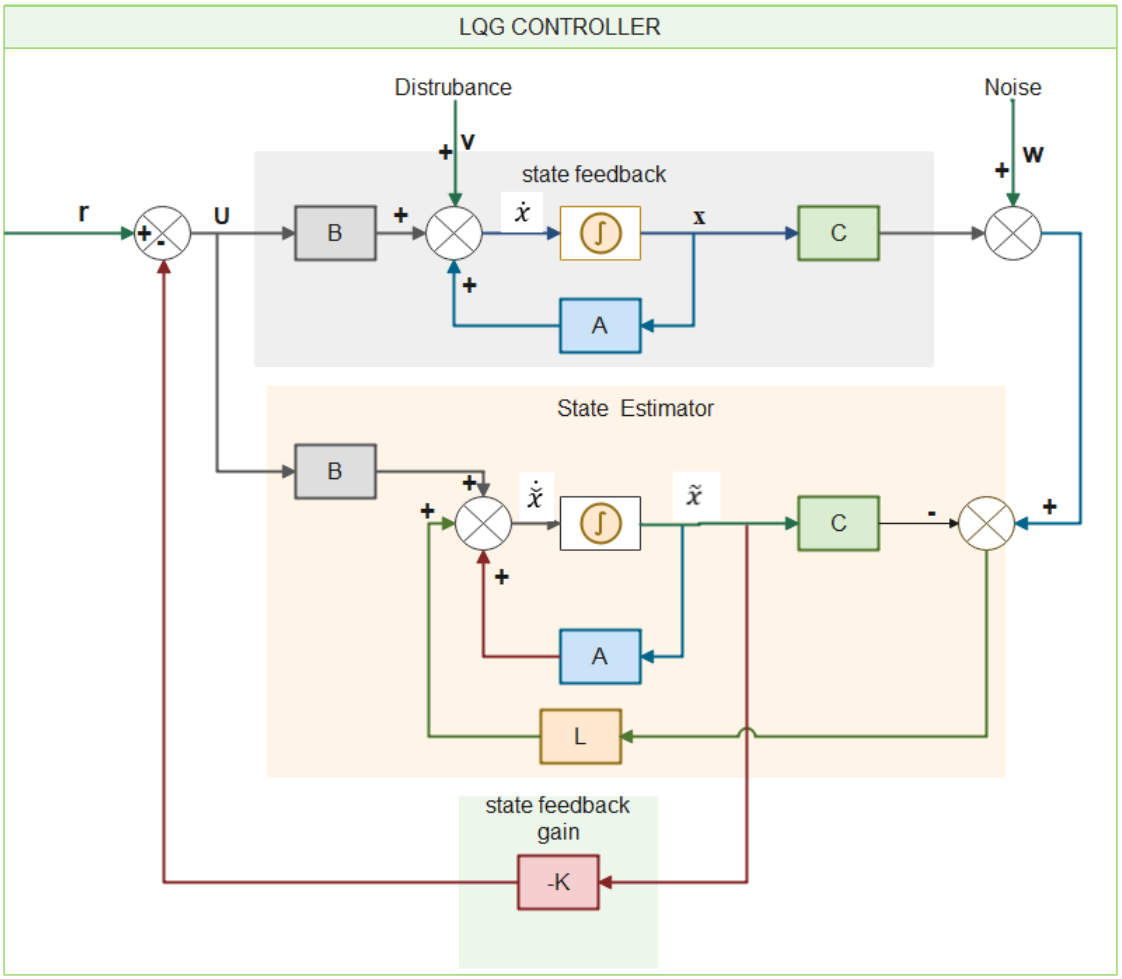


Figure (4.4) LQG Control block diagram

From above Figure 4.4,$u$ is represent the control input,$y$ is the measured control output,$x$ is the state vector of state variables,$A$ is the state matrix,$B$ is the input matrix, $C$ is the output matrix,$V$ is the disturbance input,$W$ is the measurement noise,$L$ is the feedback Kalman filter gain in form of state space and $K$ is the state feedback gain. A state observer is obtained by producing a state estimate $\hat{x}$.

### 4.3.2 Linear Quadratic Regulator (LQR) Controller

The objective of the first stage is linear quadratic regulator typical technique for determining the state feedback gain in a closed-loop system. It is the best regulator for relocating open-loop poles to obtain a stable system with optimal control and the least cost for given cost function weighting matrices. That is when employing the optimal regulator technique freedom of choice is lost for both discrete-time and continuous-time systems because there are some locations where the poles cannot be assigned to obtain a positive definite Riccati

equation solution. The advantage of LQR is that it can improve the system performance by managing the motor speed and position and to minimize the energy used by the control action itself to a minimum, the magnitude of the control action is frequently included in this amount. At its foundation, the LQR algorithm is simply an automated method of locating an acceptable state feedback controller and obtaining a matrix K the matrix that defines the controller in such a way that it minimizes a cost function. Therefore, the selection of K is an optimization problem. The purpose of the LQR design optimization issue is to find a matrix K that defines the controller in such a way that the cost function is minimized.
A state feedback system is a proper selection feedback system structure underlying the BLDC motor design control system. The BLDC motor drive system's stability is a major concern. If the state variables are known, then they can be used to design a feedback controller such that the input becomes:

$$U = -Kx \tag{4.10}$$

It is necessary to measure and use the state variables of the system to control the speed of the BLDC motor. The state variable must be changed in the state-space form then the state space representation of LQR as shown in figure 4.5[33].

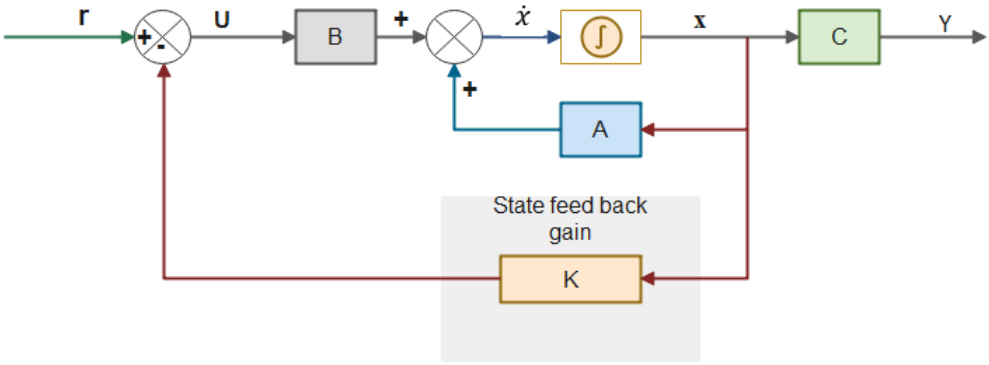


Figure (4.5) State space control of LQR controller.

This design state variable feedback control method gives enough information about the stability of the BLDC drive system. The linear quadratic regulator system considered in this study is described as follows

$$A^T P + PA - PBR^{-1}B^T P + Q = 0 \tag{4.11}$$

This equation is 4.11 called the Algebraic Ricatti Equation.For a symmetric positive-definite

matrix $P$. The regulator gain K is given by:

$$K = R^{-1}B^{T}P \tag{4.12}$$

Therefore,the choice of K is an optimization problem.The optimization problem of the LQR is to Minimizing the cost function.

$$J = \int_{0}^{\infty} ((x^{T}(t)QX(t) + U^{T}(t)RU(t))dt \tag{4.13}$$

is subject to

$$\dot{x} = Ax(t) + Bu(t) \tag{4.14}$$

Where $Q$ and $R$ are the weight matrix the optimization problem of LQR gain.The signal $x(t)$ or $u(t)$ is more important in the optimization problem. The actual values of $Q$ and $R$ are not related and the ratio of their magnitudes is a matter of factors that affect the optimization priority. Choose one of the $Q$ and $R$ practical and simple way is to define $Q$ is the identity matrix and change the value of $R$ until the expected result is obtained.

### 4.3.3 Linear Quadratic Estimator (LQE) Controller

The Kalman filter is also known as linear quadratic estimation (LQE). It is optimal that uses a series of measured values observed over time including noise and other inaccuracies.It produces estimates of unknown variables that seem to be better than those based on a single those measured Kalman filter [34],[35],[36]. Has several applications in technology some applications are navigation, vehicle control, and guidance. The Kalman filter is a widely used concept in time analysis and is used in fields such as signal processing.
The state equations for the state estimator can be derived in a variety of methods. The estimator state equations can be modeled as a model of the actual system plus a correction term based on the measured output and an estimate of what that output should be and the state estimator is modeled based on the state space equation[37].

$$\begin{aligned} \dot{\hat{x}(t)} &= A\hat{x} + Bu(t) + L(y(t) - \hat{y(t)}) \\ \hat{y(t)} &= C\hat{x(t)} + Du(t) \end{aligned} \tag{4.15}$$

Where $L$ is the observer's $nxm$ gain matrix.The state equation 4.15 can be considered as a model for the actual state equation 4.14 with the true state $x(t)$ to substitute by the estimate

$x(t)$ and a correction term equal to the difference between the actual measured output $y(t)$ and its estimate $y(t)$.

### 4.3.4 Design of Linear Quadratic Gaussian Controller for Speed Control of the BLDC Motor

To design the LQG Controller the plant model requires the state-space model and to use the BLDC motor state space represents to identify the state, where the input is voltage and output is speed from the state variable of the speed of the BLDC motor. Then from the modeling BLDC motor in above equation 3.7 and 3.12 to get the state space representation of BLDC motor is :

$$\begin{aligned} \frac{di}{dt} &= \frac{v}{L} - \frac{Ri}{L} - \frac{e}{L} \\ \frac{d\omega}{dt} &= \frac{T_e}{J} - \frac{B\omega}{J} - \frac{T_L}{J} \end{aligned} \tag{4.16}$$

Where $T_e = iK_t$ ,$e = K_b\omega$ ,and $T_L = 0$ then equation4.16 become:

$$\begin{aligned} \frac{di}{dt} &= \frac{v}{L} - \frac{R}{L}i - \frac{K_b}{L}\omega \\ \frac{d\omega}{dt} &= \frac{K_t}{J}i - \frac{B}{J}\omega \end{aligned} \tag{4.17}$$

**Motor Parameter Selection**

The basis for all the simulations is an eight-pole, 50 Hz three-phase BLDC. The rated power of 7.5 KW and rated torque is 45 Nm are used for simulation. The simulation model is developed in MATLAB/SIMULINK. The simulation parameters for the BLDC motor are shown in the table 4.1 [38].

Table (4.1) Electrical and mechanical parameter of the motor

| **Parameter** | **unit** | **Value** |
|---|---|---|
| Stator Resistance ($R_a$) | $\Omega$ | 0.95 |
| Torque constant ($K_t$) | $N.m/A$ | 0.095 |
| inductance ($L$) | H | 0.00144 |
| Back emf constant ($K_b$) | $V/rpm$ | 9.9484 |
| damping ($B$) | $N.m.s$ | 0.00001 |
| No. of pole pair ($p$) | $-$ | 4 |
| Inertia ($J$) | $Kg/m^2$ | 0.0019 |

Let $x_1$=$\omega$ and $x_2$ =$i$ from the above equation 4.17 to get:

$$\begin{aligned} \dot{x_1} &= -\frac{K_b}{L}x_1 + \frac{R}{L}x_2 \\ \dot{x_2} &= -\frac{B}{J}x_1 - \frac{K_t}{J}x_2 + \frac{v}{L} \end{aligned} \tag{4.18}$$

Then to substitute from above table 4.1 motor parameter in to equation 4.18 the state space model for BLDC motor become:

$$\begin{aligned} \dot{x_1} &= -0.005x_1 + 50x_2 \\ \dot{x_2} &= -6908.6x_1 - 659.78x_2 + 6694.4u \\ y &= x_1 \end{aligned} \tag{4.19}$$

The state space representation of BLDC motor in matrix form is

$$\begin{aligned} \begin{bmatrix} \dot{x_1} \\ \dot{x_2} \end{bmatrix} &= \begin{bmatrix} -0.005 & 50 \\ -6908.6 & -659.78 \end{bmatrix} \begin{bmatrix} x_1 \\ x_2 \end{bmatrix} + \begin{bmatrix} 0 \\ 694.4 \end{bmatrix} u \\ y &= \begin{bmatrix} 1 & 0 \end{bmatrix} \begin{bmatrix} x_1 \\ x_2 \end{bmatrix} \end{aligned} \tag{4.20}$$

In the LQG control design to use the plant state-space model of the state is a regulator to zero so we can use the error dynamic model of the state space. Then error dynamic model become

$$\begin{aligned} e(t) &= \omega_{ref} - \omega_{actual} \\ \dot{e}(t) &= -\dot{\omega}_{actual} \end{aligned} \tag{4.21}$$

Let $e(t)$=$Z_1$ and $\dot{e}(t)$=$\dot{Z}_1 = Z_2$ and then from above equation 4.21 to calculate the error dynamic model for BLDC in the form of state space .

$$\begin{bmatrix} \dot{Z}_1 \\ \dot{Z}_2 \end{bmatrix} = \begin{bmatrix} 0 & 1 \\ -345433 & -659.78 \end{bmatrix} \begin{bmatrix} Z_1 \\ Z_2 \end{bmatrix} + \begin{bmatrix} 0 \\ 34720 \end{bmatrix} u$$
$$y = \begin{bmatrix} 1 & 0 \end{bmatrix} \begin{bmatrix} Z_1 \\ Z_2 \end{bmatrix} \tag{4.22}$$

## 4.4 Particle Swarm Optimization (PSO) Algorithm

TThe particle swarm optimization algorithm is one of the random algorithms based on the group. The optimization technique proposed by Eberhart and Kennedy (1995) [39]. The PSO algorithm simulates the behavior of social animals including insects, cattle, birds, and fish. This flock of birds or fishes created cooperation with their wisdom and was also influenced by collective behavior in the pursuit of food. Each member of the flock continued to adjust their search behavior according to their own other members' learning experience [40]. Therefore, if a particle or a bird finds the correct path or shortest distance to the food source, others can immediately follow the path despite their long distances between groups.

The social behavior of flocks of birds or schools of fish inspired particle swarm optimization, which is a population-based stochastic optimization technique. PSO helps in the solution of optimization problems.PSO refers to each solution as a "bird" in the "particle" search space. All particles have fitness values that the fitness function evaluates to optimize them, as well as velocities that direct their flight. Through the problem space, the particles follow the current optimum particles. PSO starts with a set of random particles and then looks for optimization by updating generations. Every particle is updated in each iteration by comparing these two "best" values. The first is the best solution (fitness) thus far. Personal best is the name given to this value. The best value obtained so far by any particle in the population is another "best" value recorded by the particle swarm optimizer. This best value is referred to as gbest, which stands for "global best". In d-dimensional space the $i_{th}$ particle is represented as $X_i$=$(X_i1, X_i2, ..., X_id)$and velocity $V_i$ is the N-dimensional search space.Where $i$ represents the $i^{th}$ particle and $N$ denotes the dimensions of the search space or the number of unknown variables. The particles are moving through the problem space attempting to reach the population of the actual optimum value. Each particle will make a point of remembering their best position to present, which is referred to as personal best(Pbest). There are many Pbest for each particle in the swarm at the same time. But the particle with the best value obtained thus far, as well as the greatest fitness is referred

to as the swarm's global best (Gbest). The particles will update their velocity and position to the current best value after obtaining the two best values. The following is a summary of the main steps in the particle swarm optimization and selection process:

1. Initialize a population of particles in d-dimensions with random positions and velocities.
2. Each particle in the swarm is examined for its fitness.
3. The fitness of each particle is compared to its previous best fitness (Pbest) in iteration.If the current value is better than Pbest .Then Pbest is set equal to the current value and the Pbest location equal to the current location in the d-dimensional space.
4. Pbest of each particle is compared and the swarm global best location is updated.
5. The particle of velocity and position is updated according to equations 4.23 and 4.24 respectively, [39].

$$V_k^{i+1} = WV_i^k + C_1 r_1 (Pbest_i^k - X_i^k) + C_2 r_2 (Gbest_i^k - X_i^k) \tag{4.23}$$

$$X_i^{k+1} = x_i^k + V_i^{K+1} \tag{4.24}$$

The iteration mechanism of any particle in each generation is shown in Fig 4.6[39]. When looking at the velocity update formula from a sociological standpoint we can see that the first part is the effect of the particle's past velocity. It indicates that the particle has faith in its current moving condition and moves inertially according to its velocity. Hence, the name inertia weight. The second element is referred to as the "cognitive" item. It is determined by the distance between the particle's current position and its optimal position.

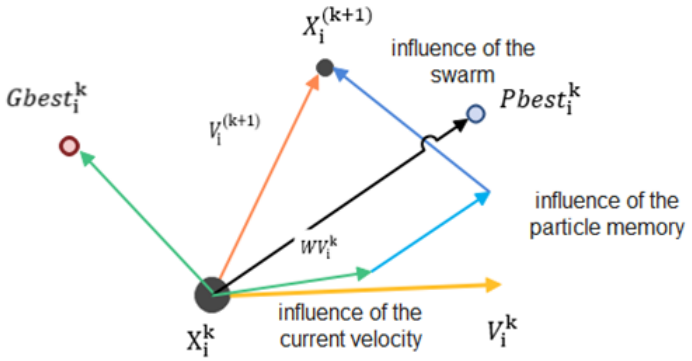


Figure (4.6) Iteration scheme of the particles

It refers to a particle movement as a result of its own experience. As a result,$C_1$ is known as the cognitive learning factor (also known as the cognitive acceleration factor). The other is known as the social factor. it is based on the distance between the particle's current position and the global(or local)ideal position in the swarm. It refers to the sharing of knowledge and cooperation among particles specifically particle movement based on the experiences of other particles in the swarm. Because the value $C_2$ simulates the movement of a good particle through cognition. It is known as the social learning factor(also known as the social acceleration factor). The parameters of the PSO search and minimization algorithm are as follows: $W$ is the inertia weight factor that controls the exploration and exploitation of the search space by dynamically adjusting velocity. The resolution and fitness of search depend on $V_i$.If $V$ is too high the particles will move beyond a good solution. If $V$ is too low the particles will be trapped in local minimal. The constants $C_1$ and$C_2$ ) are termed known as cognition and social components respectively. These are the acceleration constants that influence a particle of velocity.

### Flowchart of PSO

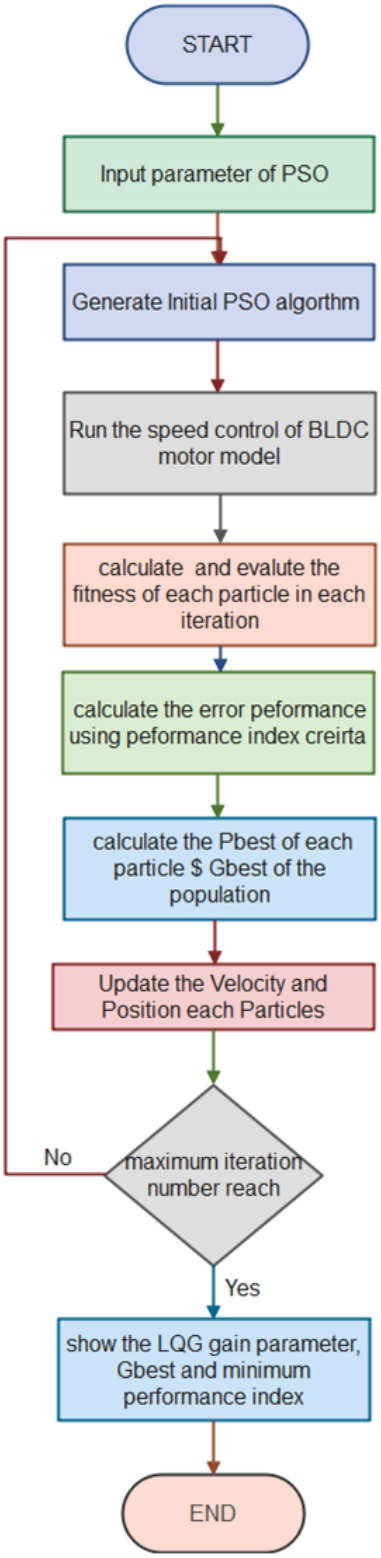


Figure (4.7) Flowchart of PSO

## 4.5 Particle Swarm Optimization Tuned Linear Quadratic Gaussian Controller

The Simulation of tuned LQG Controller with PSO for Brushless dc of speed control is based on the block diagram shown in the figure 4.8. This thesis work describes the Modeling of Brushless Dc motor, the control strategy for LQG controller tuned with particle swarm optimization, to control the gate signal, phase current, back emf, and the torque of the BLDC motor using speed control.

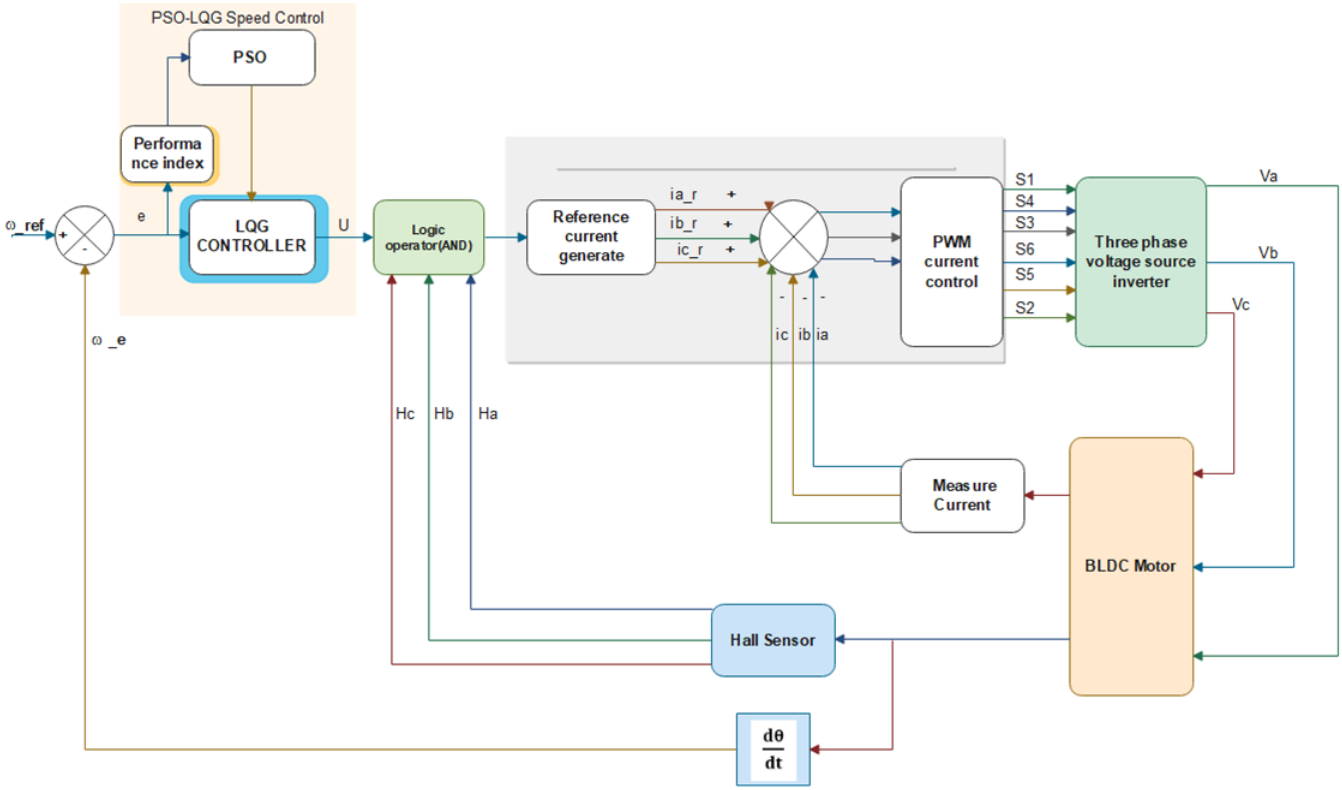


Figure (4.8) General Block diagram speed control of BLDC motor LQG tune with PSO controller

The simulation model of the whole system shown on the block diagram is developed and simulated on MATLAB/ SIMULINK.In this study is the core simulation environment containing controller model, Motor model, and Inverter block. The BLDC block on the general block diagram of the above Figure4.8 shows that phase current and rotor speed are the available feedback for control. The current command is implemented by the inner loop, whereas the speed command is implemented by the outside loop. The speed control is done by the LQG-PSO controller. The torque command signal is obtained from the speed error and the torque command output is used to generate the pulse width modulated signal to crate gate

switch for each phase switch by obtaining the phase current error.

The weighting matrices of the LQG have several parameters to be selected. This allows working intuitively with complex characteristics such as noise, uncertainties, and saturation just by inserting them into the simulation used for PSO. This work shows a convergence analysis of PSO for this LQG problem. To obtain solutions from different trials resulted in LQG gains contained in a well-defined region to suggest that optimal was reached. Simulation results have also shown good dynamic behavior with the LQG-PSO strategy. Which has outperformed a cascade PI controller for different reference speeds. Linear Quadratic Gaussian (LQG) controllers configured in a cascade loop with weighting matrices optimized by PSO, the goal is to obtain performance for reference tracking as well as against disturbances, uncertainties, and noise.

To find the LQG controller gain parameter the depends upon the lower bound and upper bound to initiate the parameter value of PSO to increase and the number of iteration. It is get a minimum error value and the best optimal gain parameter. In the appendices section, C show that the PSO algorithm for the optimization techniques from this result to get the best gain parameter of LQG controller.

**Fitness Function**

Integrated absolute error (IAE), integrated time weight square error (ITSE), and integrated squared error (ISE) are the most commonly used performance criteria in PSO tune LQG controller design approaches, and they may all be evaluated analytically. This performance criterion has both advantages and disadvantages. Because the ISE performance criterion weights all mistakes equally regardless of time, it can result in a response with a small overshoot but a long settling time. Although the ITSE performance criterion can compensate for the ISE criterion's shortcomings. The derivation processes of the analytical formula are complex and time-consuming. The IAE, ISE, ITAE, and ITSE performance criterion formulas are as follows:

$$\begin{aligned} ISE &= \int_0^\infty e^2(t)dt \\ ITSE &= \int_0^\infty te^2(t)dt \\ IAE &= \int_0^\infty |e(t)|dt \\ ITAE &= \int_0^\infty t|e(t)|dt \end{aligned} \tag{4.25}$$

Let the value of x=z i.e $z_1 = x_1$ ,and $z_2 = x_2$ the equation become.

$$\begin{aligned} U &= -Kz \\ U &= \begin{bmatrix} -K_1 & -K_2 \end{bmatrix} \begin{bmatrix} z_1 \\ z_2 \end{bmatrix} \end{aligned} \tag{4.26}$$

The state space equation for

$$\dot{x} = Az(t) + Bu(t) \tag{4.27}$$

Then to substitute equation 4.22 in to4.27 become:

$$\begin{aligned} \dot{z_1} &= z_2 \\ \dot{z_2} &= -345433z_1 - 659.78z_2 + 34720(k_1 z_1 - k_2 z_2) \\ y &= z_1 \end{aligned} \tag{4.28}$$

Then equation4.28 becomes:

$$\begin{aligned} \dot{z_1} &= z_2 \\ \dot{z_2} &= (-345433 - 34720k_1)z_1 + (-659.78 - 34720k_2)z_2 \\ y &= X_1 \end{aligned} \tag{4.29}$$

And the state estimator equation become

$$\begin{aligned} \dot{\hat{z_1}} &= \hat{z_2} \\ \dot{\hat{z_2}} &= (-345433 - 34720k_3)\hat{z_1} + (-659.78 - 34720k_4)\hat{z_2} \\ y &= \hat{z_1} \end{aligned} \tag{4.30}$$

The gain parameters $k_1$ and $k_2$ are the state feed gain. The gain parameter $k_3, k_4$, are state estimator gains.The gain parmater $k_5$ is the kalman fiter gain.It can yield a good step response that will result in performance criteria minimization in the time domain. These performance criteria in the time domain include the overshoot, rise time, settling time, and steady-state error.

The value of $k_1, k_2, k_3, k_4$ and $k_5$ corresponding to the best solution obtained is used in the simulink block diagram shown in the figure A.2.Even though the design of $k_1, k_2, k_3, k_4$, and $k_5$ is carried out assuming that there is no change in reference speed the values of $k_1, k_2, k_3, k_4$ ,and $k_5$ obtained through PSO are now used to study the system's response.The following table4.2 is PSO parameters are used to verify the performance of the PSO-LQG controller

parameters.The performance criterion based on the absolute error the gain parameter become value $k_1 = 3.5, k_2 = 1.5, k_3 = 3.35, k_4 = 5.5$ ,and $k_5 = 2.33$.

Table (4.2) PSO Parameter used tuned LQG controller

| **Parameter** | **Value** |
|---|---|
| Acceleration coefficient($c_1$), | 1.5 |
| Acceleration coefficient($c_2$) | 1.5 |
| population size | 10 |
| iteration | 5 |
| number of variable | 5 |
| lower bound | 1 |
| upper bound | 10 |
| inertia weight | 0.8 |

## 4.6 Motor Power Rating Calculation and Motor Parameter Selection

**Motor Power Rating Calculation** The electric motor used in an electric vehicle must produce the appropriate power and other characteristics necessary for traction. The important task is to choose the appropriate motor classification based on the carrying load. The dynamics of vehicles are considered to be the choice of the appropriate electric motor that will provide the required power and torque for traction. Choosing the right rating also helps in using the right size electric motor as the size of the motor depends on the rating. Therefore, to achieve all the traction properties in the compact size the appropriate choice of motor rating based on the load must be made, [41],[42].

The output characteristics of a vehicle are determined by an electric motor in terms of power,torque,and speed.The electric motor selected to drive a vehicle must be able to produce enough power and torque to resist the force exerted on the vehicle by the load and other opposing forces.

Selected electric automobile(Tesla Model S 75) with the parameters listed on the table 4.3[41] is used for calculating the required ratings of the motor.

Table (4.3) Parameters used for motor rating calculation, Tesla Model S 75

| **Paramter** | **Value** |
|---|---|
| Curb weight, $Kg$ | 1500 |
| Rated speed, $km/hr$ | 80 |
| Frontal area of the car, $m^2$ | 2.43 |
| Battery pack output, $V$ | 400 |
| Time to accelerate to rated speed, $sec$ | 10 |

### Road Load, Tractive Force and Power, Transmission

According to [43],the road load consists of the gravitational force ($F_{gradient}$), rolling resistance ($F_{rolling}$) of the tires and the aerodynamic drag force ($F_{aerodynamic\,drag}$). The tractive force $F_{acceleration}$ provided by the main propulsion unit of the vehicle must overcome the road load ($F_{rolling} + F_{gradient} + F_{aerodynamicdrag}$) to propel the vehicle forward at a desired velocity.

$$F_{total} = F_{rolling} + F_{gradient} + F_{aerodynamicdrag} + F_{acceleration} \tag{4.31}$$

Where:

$$\begin{aligned} F_{total} &- \text{Total force} \\ F_{rolling} &- \text{Force due to rolling resistance} \\ F_{gradient} &- \text{Force due to gradient resistance} \\ F_{aerodynamic\,drag} &- \text{Force due to aerodynamic drag} \\ F_{acceleration} &- \text{force required to reach predefined speed} \end{aligned}$$

$F_{total}$ is the total tractive force that the output of motor must overcome, in order to move the vehicle to the desired velocity.

### 1. ROLLING RESISTANCE

Rolling resistance is the resistance offered to a vehicle by the contact of tires with the road. The formula for calculating the force due to rolling resistance is given by the equation, [43].

$$F_{rolling} = C_{rr} * m * g * \cos\alpha \tag{4.32}$$

Refer tables 4.3 4.4 for the name and values of the variables in the above equation.

Power required to overcome the rolling resistance is:

$$P_{rolling} = (F_{rolling} * \frac{V}{3600})KW \tag{4.33}$$

Using equations 4.32 and 4.33 and the value of the constants in 4.4, the $F_{rolling}$ value becomes 234.09 N and the power required to overcome this rolling resistive force $P_{rolling}$ becomes 5.2 KW considering the parameters value of table 4.3 and 4.4.

### 2. GRADIENT RESISTANCE

Gradient resistance of the vehicle is the resistance offered to the vehicle while climbing a hill or flyover or while traveling in a downward slope. The angle between the ground and slope of the path, as shown in the figure 4.9 is represented as $\alpha$,

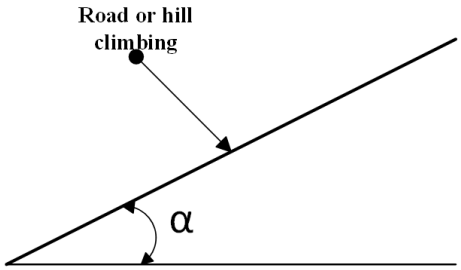


Figure (4.9) Angle between the ground and the road

The equation for calculating the gradient resistance force is given by equation 4.34,

$$F_{gradient} = \pm M * g * \sin\alpha \tag{4.34}$$

Since this model considers an electric car runing on a flat ground. Which implies the angle $\alpha = 0\,\text{deg}$. Therefore, the gradient resistant force becomes zero (i.e. $F_{gradient} = 0N$). Also the power required to overcome this gradient resistance force becomes zero.

### 3. AERODYNAMIC DRAG

The resistive force provided by the viscous force pushing on the vehicle is known as aerodynamic drag. It is mostly determined by the vehicle's shape. The formula for calculating the aerodynamic drag is given by equation, [43].

$$F_{aerodynamic\,drag} = 0.5 * C_A * A_f * \rho * (V + V_0)^2 \tag{4.35}$$

Power required by the vehicle to overcome the aerodynamic drag force can be calculated by:

$$P_{aerodynamic\,drag} = F_{rolling} * \frac{V}{3600} \tag{4.36}$$

Using equations 4.35 and 4.36, the $F_{aerodynamic\,drag}$ value becomes $187N$ and the power required to overcome this aerodynamic drag force $P_{aerodynamic\,drag}$ becomes $4.158KW$ by using the following parameters values listed in the tables 4.3 and 4.4.

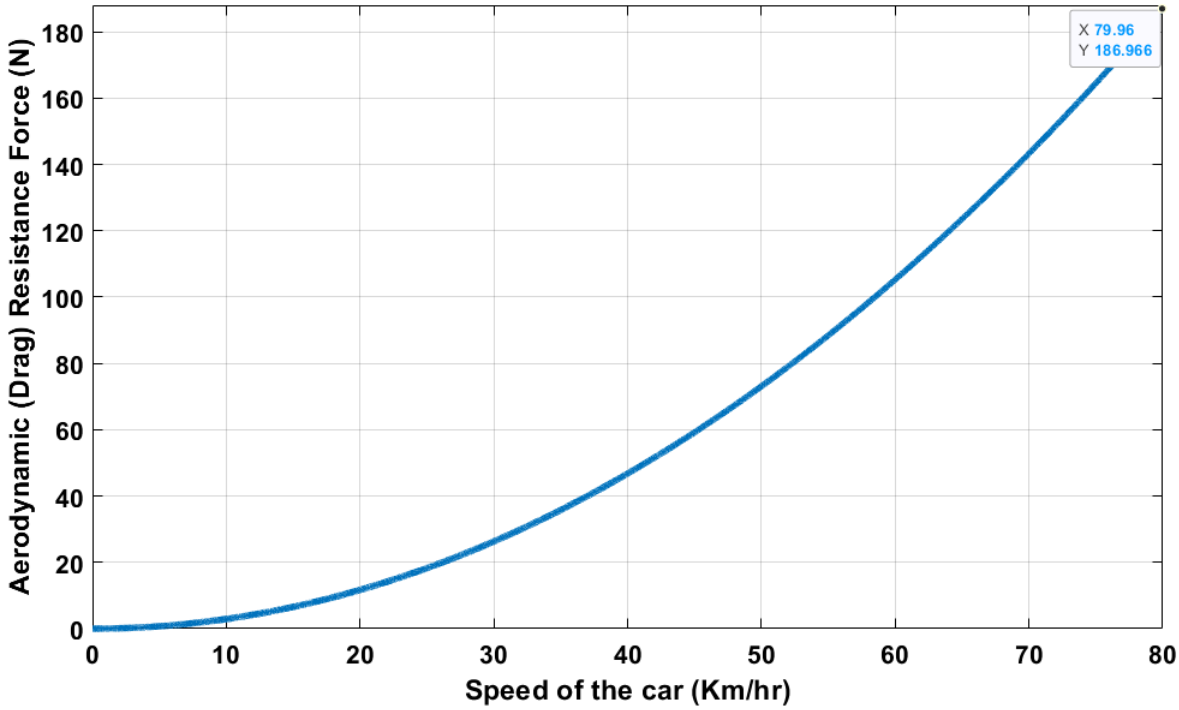


Figure (4.10) Aerodynamic dragging force versus speed of the car in km/hr

The aerodynamic force increases with the square of the car speed as shown in Figure 4.10.The drag force is directly proportional to the total of the wind and the square of the car speed, as shown by Equation 4.35.The force increases from 0 to 187N as the car speed climbs from 0 to 80 km/hr.The wind speed is believed to be zero because it is so low in comparison to the car's speed.

**4. ACCELERATION FORCE**

The acceleration force is the force that assists the vehicle in reaching a predetermined speed from a standstill in a given amount of time. The acceleration force and the motor torque have a direct relationship. The higher the torque, the less time it takes for the vehicle to reach a particular speed. The acceleration force is proportional to the vehicle's mass [42],[44].

Acceleration force and Power required to reach rated speed starting from rest is calculated using equations 4.37 and 4.38.

$$F_a = m * a \tag{4.37}$$

$$P_a = F_a * \frac{V}{3600} \tag{4.38}$$

Before getting into the calculation of the acceleration force($F_a$) and the required power, [43].First calculate the acceleration, $a$, using equation 4.39 by assuming the vehicle took $10sec$ to reach rated speed ($80km/hr$) from starting form rest.

$$a = \frac{V}{t} \tag{4.39}$$

The resulting acceleration of the car becomes $2.22m/s^2$. And the acceleration force obtained is $3330N$ and the power required becomes $74KW$.

These are the four main forces which act on the vehicle when it accelerates to rated speed starting from rest. Therefore, the total tractive power (the sum of all the powers obtained above) required to move the vehicle becomes $83.35KW$,

But electric motor with output power rating of $83.35kW$ should not be selected. The losses due transmission of power to the wheel must be included. Therefore, the mechanical power output $P_{mech}$ required to drive the vehicle is given by equation 4.40.

$$P_{mech} = P_{total}/\eta \tag{4.40}$$

Where, $\eta$ = efficiency of the transmission gear system.

Let us take the efficiency of the transmission system to be 0.85 and the resulting mechanical power output required becomes $84KW$ approximately.

Therefore, the illustration of selection of power rating of an electric motor for an electric car of gross weight $1500kg$ the output power rating of $84kW$ has to be selected. In this way, power rating required to drive an electric vehicle of particular load is calculated.

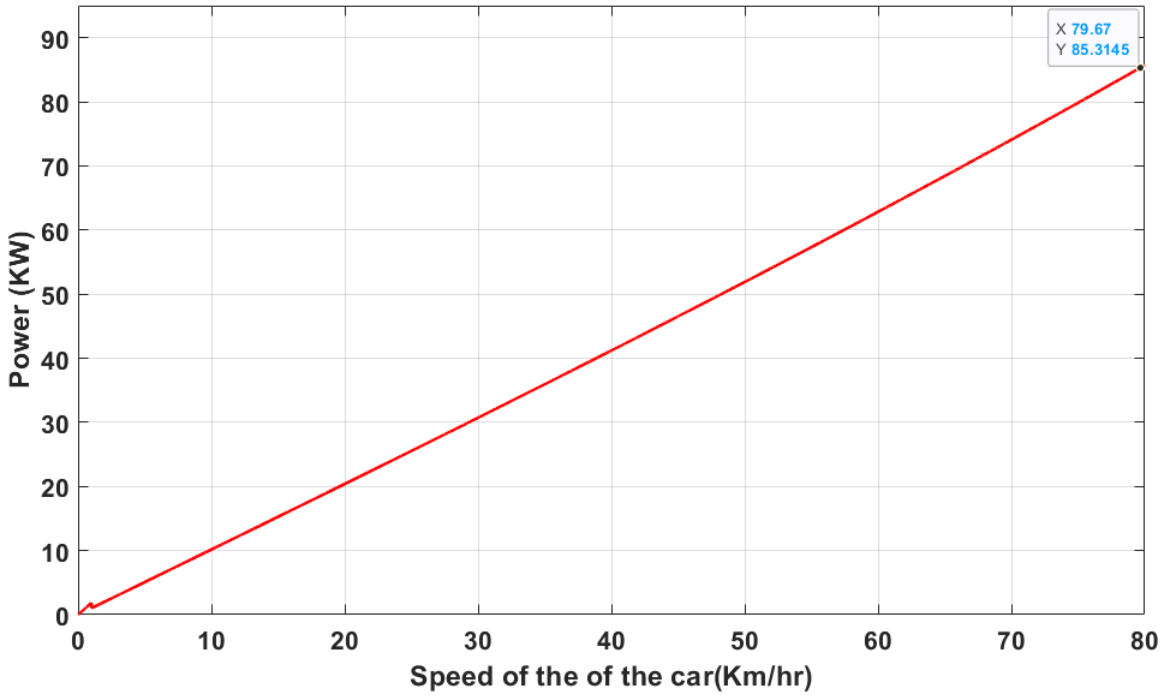


Figure (4.11) Power versus speed of the vehicle

In Figure 4.11,a vehicle with its full load accelerates at $2.22m/s^2$ on a flat road and the power required to overcome the forces is $84kW$.

### Motor Speed and Torque Rating

Next let's discuss the motor's speed and torque ratings calculation for this particular electric vehicle application. Assuming the EV tire of radius ($r = 19$") or diameter ($d = 0.48m$) and the car moving with towards a rated speed of $22.22m/s$, which is also the speed of the rim of the tire.

The angular velocity of the tire (wheel) is obtained to be equal to $\omega_{tire} = 92.58rad/sec$ and $N_{wheel} = 884.55rpm$ use equations 4.41 and 4.42 for the calculation.

$$\omega_{tire} = \frac{V}{r} \tag{4.41}$$

$$N_{wheel} = \omega * \frac{60}{2\pi} \tag{4.42}$$

The motor $rpm$ considering the gear transformation ratio becomes $N_{motor} = 9,730rpm$ using

the following equation,

$$N_{motor} = gear\ ratio * N_{wheel} \tag{4.43}$$

Where the the $gear_ratio = 1:11$.

Finally, the torque (motor torque) required to drive the vehicle to the speed $80km/h$ given the motor power rating $84KW$, is calculated as,

$$T_m = \frac{9.55 * P_{mech}}{N_{motor}} \tag{4.44}$$

Therefore the resulting torque rating the motor with $84KW$ of rated power is $82,48Nm$ which is capable of driving the vehicle to the rated speed of $9730rpm$.

**Summery**

Constants used in the entire calculation of the rated power, rated speed and rated torque of the motor for the EV application are listed in the table 4.4[41],[7]

Table (4.4) Constants used in the entire calculation of the motor ratings

| **Constants** | **Symbol** | **Value** |
|---|---|---|
| Gear Ratio | $GR$ | 1: 11 |
| Power Factor | $pf$ | 0.8 |
| Gravity $(m/s^2)$ | $g$ | 9.81 |
| Transmission efficiency (%) | $\eta$ | 85 |
| fluid density of an air $(kg/m^3)$ | $\rho$ | 1.2 |
| The angle between the road and the ground $(degree)$ | $\alpha$ | 0 |
| dragging coefficient of a modern car | $C_A$ | 0.26 |
| coefficient of rolling resistance of a fair asphalt | $C_{rr}$ | 0.01 |

The resulting rated power, rated speed and rated torque of the BLDC are $P_{mech} = 84KW, N_{motor} = 9730\ and\ T_m = 82Nm$ respectively.

# Chapter 5

# Simulation Results and Discussion

In this chapter describe the results obtained from investigating the complete PSO tuned LQG based control model along with the discussion are presented.First the speed performances and characteristics under different load and no load operating conditions,the effect of disturbance,braking operation is provided. Finally the comparisons the performance speed based on the PSO-LQG and PI controller will be illustrated.

## 5.1 Speed Tracking Performance of PSO Tuned LQG Controller

The proposed PSO-LQG controller based drive system control model tracks the constant reference input.This shows the tracking performance of the control model to ther reference speed. The performance criteria of the PSO-LQG contoller for speed tracking brushless DC motor at a constant speed of 1000 RPM is shown in Fig figure 5.1.In this figure 5.1the X -axis and Y-axis represented the time in second(sec)and the speed (rpm) of the BLDC motor at no-load(i.e TL=0) condition respectively.From the figure 5.1 it is seen that the rise time of the controller is about $1sec$, settling time $1.98sec$ and 0.505% is overshoot. After $1.98sec$ the motor runs at a constant speed of the preset value of $1000RPM$.

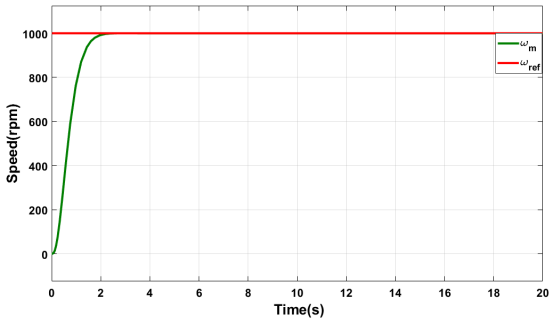


(a) Constant Reference Speed and Motor Speed

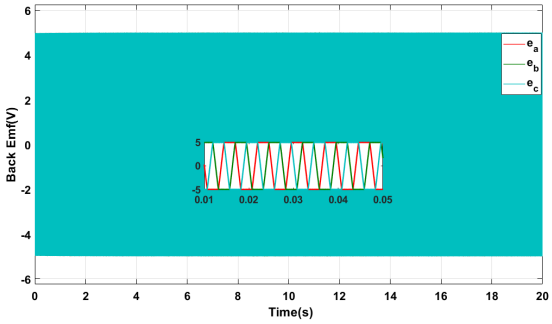


(b) Back Emf Wave form of the Motor

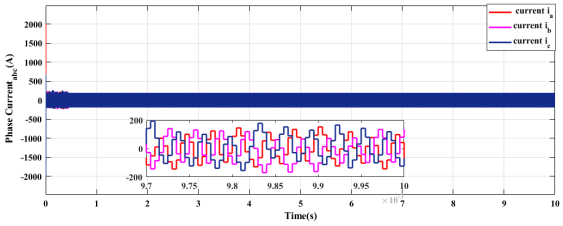


(c) Three Phase Current

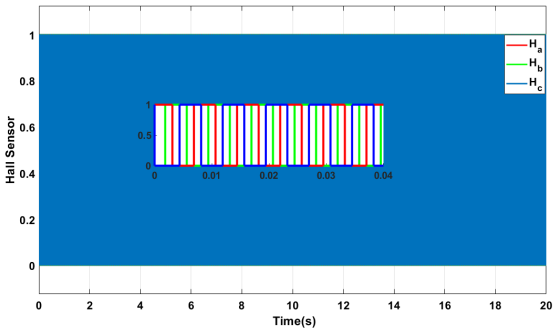


(d) Hall sensor(Position sensor)

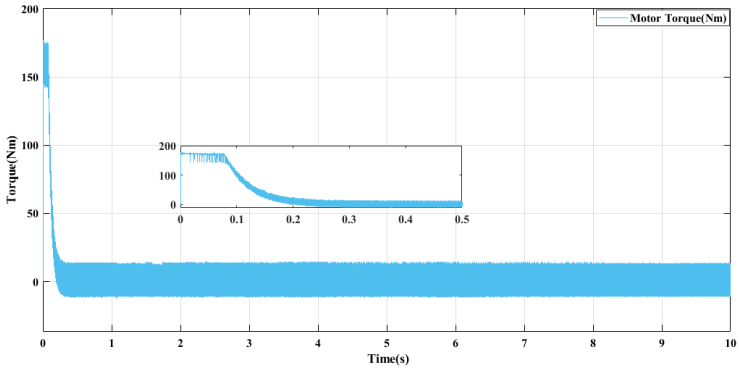


(e) Motor Torque

Figure (5.1) Speed Performance of BLDC Motor for Constant Reference Input

The simulation result shown in the figure 5.2b indicates the back emf voltages of the BLDC motor are trapezoidal induced EMFs output and the output of the figure 5.2b in the zoom section indicates the back emf wave form of BLDC motor is trapezoidal.The phase shift by $120^o$ and the magnitude of the back emf voltage is $\pm 5$.

The simulation result as shown in figure 5.1d indicate the hall sensor(position sensor) operation of the BLDC motor from the zoom section indicate three-phase signals generated from Hall sensor.

The simulation result shown in figure 5.1e show the output torque response performance of

the BLDC motor at no-load conditions.This figure 5.1e indicate the electromagnetic torque Value is measured Newton-meter of the BLDC motor at no-load condition.The start up torque in the proposed PSO-LQG controller is about 150Nm at $0.2sec$ and it is observed that the motor electromagnetic torque is fixed after $0.22sec$.Finally the BLDC motor has start high starting torque.

### 5.1.1 The Effect of Disturbance for Performance of Speed Controller

The simulation result PSO-LQG controller for speed control of the BLDC motor as shown in the figure5.2a and 5.2b under the effect disturbance.From the simulation show the effect of apply disturbance for the system.The tracking performance of the motor adds the pulse signal disturbance for 4 up to 7seconds the magnitude is 1.Then to see the effect of motor performance become oscillation for the $4-8$ seconds after that the speed tracking in reference speed(1000rpm).Finally the to conclude that the simulation results show that the PSO-LQG controller is an effective controller for band disturbance rejection.

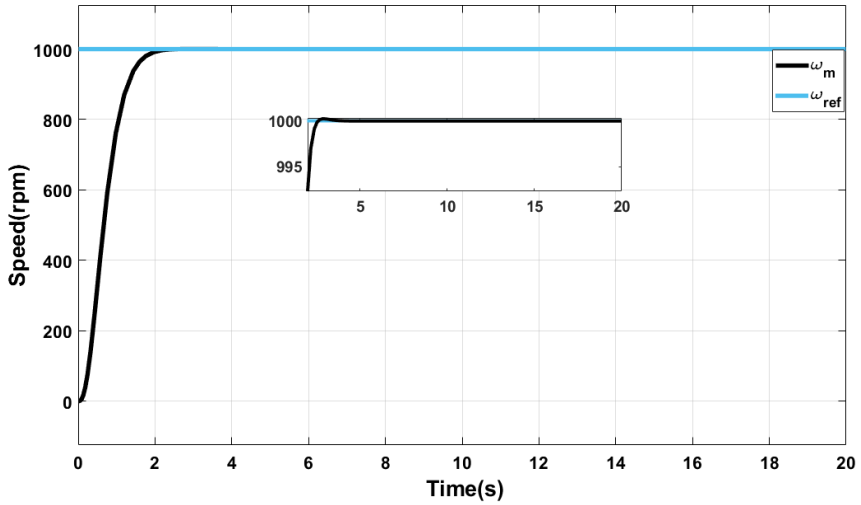


(a) Motor Speed without Disturbance Effect

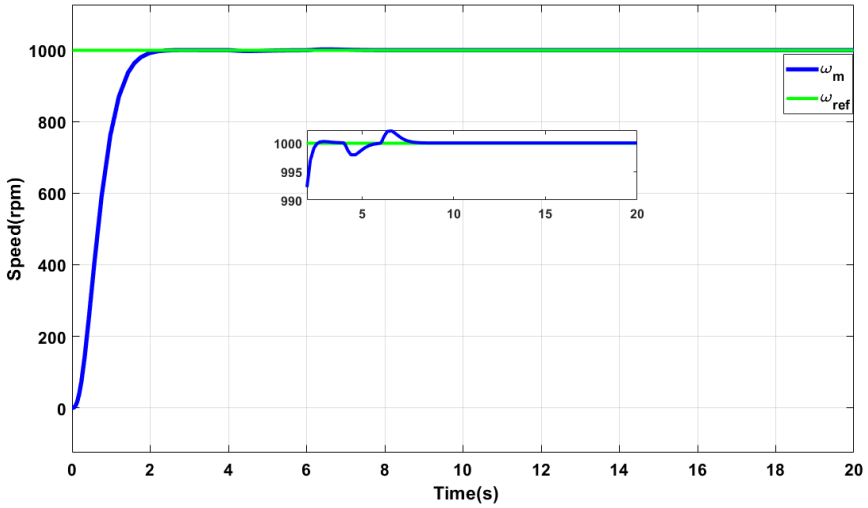


(b) Motor Speed under Disturbance Effect

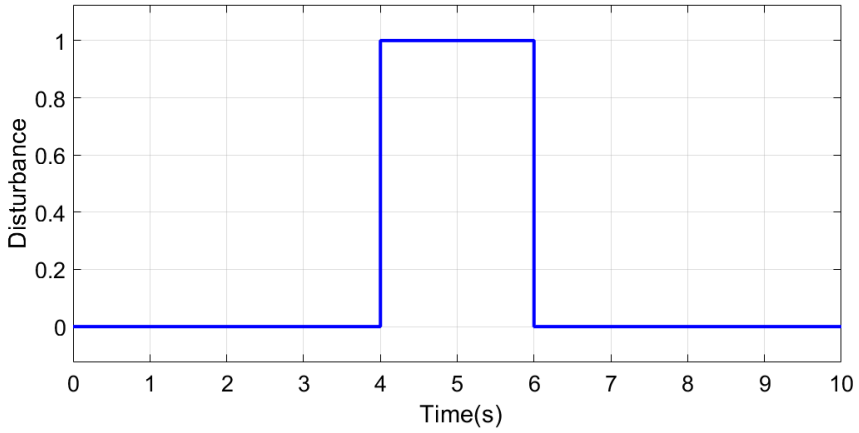


(c) Disturbance Input

Figure (5.2) Speed Performance Under the Effect of Disturbance in put

### 5.1.2 Four Quadrant Operation

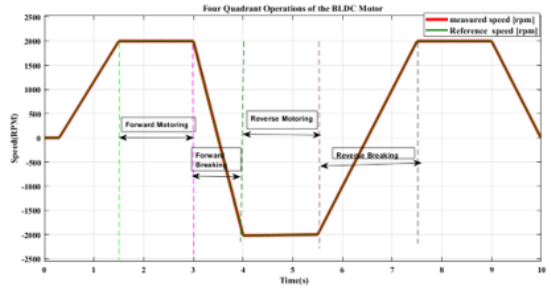


(a) Motor Speed for Four Quadrant Operation

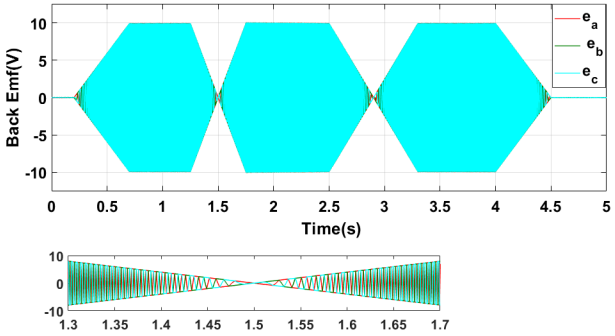


(b) Back Emf Three Phase for Four Quadrant Operation

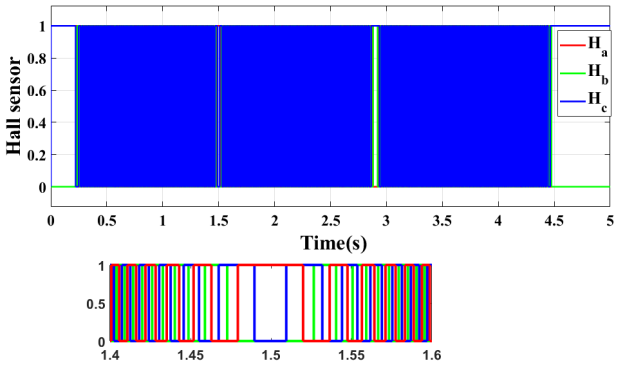


(c) Position Sensor(Hall sensor)

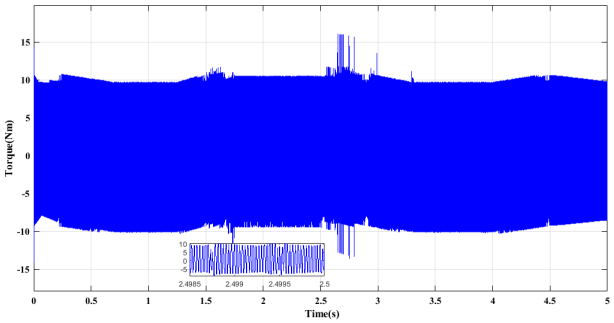


(d) Motor Torque

Figure (5.3) Under no-Load Transients and Steady State Responses for Four Quadrant Operation

Show in the figure 5.3ais the simulation results for the four quadrants operation of the motor.From time interval t between 0.75sec to 1.25sec the speed set point is 2000rpm and the applied load torque is positive then the motor operate the first quadrant namely motoring mode.During the time interval t =1.25sec to 1.5sec both the speed and load torque to the motor is negative. That is the motor is operating in the third quadrant it is namely reverse motoring.As can be seen in the Figure shown 5.3a, the actual speed tries to follow the speed set point ramp by decreasing the speed to zero and starting to speed up with a rotation in a reverse direction.From time $t = 2.5$ sec to 2.9sec positive load torque is applied to the motor. While, the speed set point is still negative.This implies that a brake is applied and that the machine is operating in the fourth quadrant it is know as reverse braking.And the simulation result shows the response of the drive system to the direction reversal speed command.As the motor drive obtains speed decreasing command at time t 1.25sec due to change mode operation the motor mode in to braking mode and after this zero slope value the negative

slop inverse tangent plot follows and continues this way as long as the required speed is in the reverse direction.

The Simulation result of the four quadrant operation of BLDC motor is shown in figure5.3b.Show that the back emf wave for BLDC motor with trapezoidal back EMF.This operation of back emf based on the Four quadrant when the time interval between $1-2$sec the braking operation is happen.From the time at 1 sec there is mode change operation mode that means motor mode operation to motor braking mode.

### 5.1.3 Tracking Capability of Controllers for reference speed variation

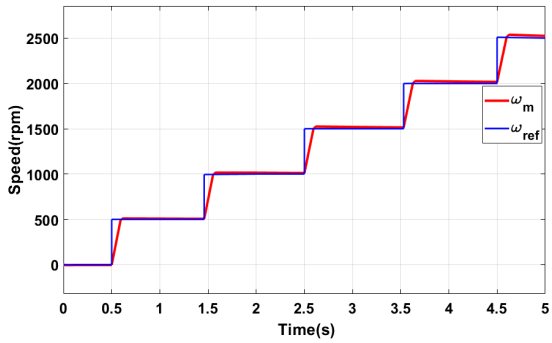


(a) Load Motor Speed

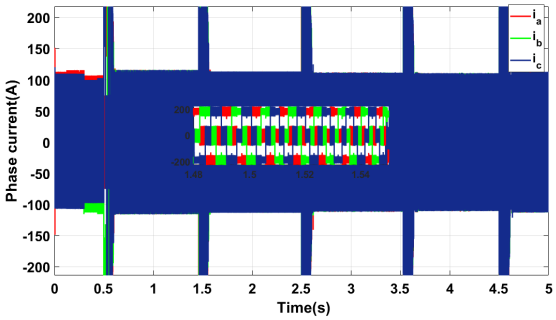


(b) Three Phase Current

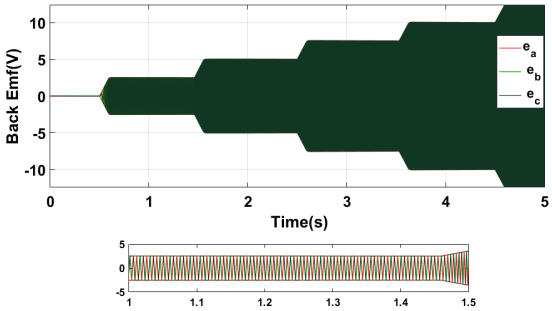


(c) Back Emf

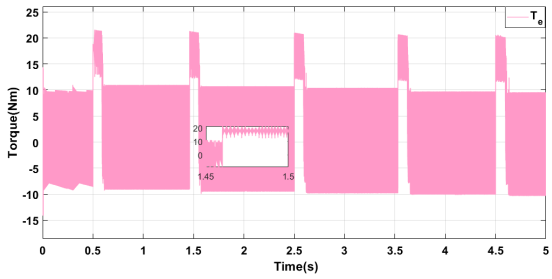


(d) Motor Torque

Figure (5.4) Increase Stair Case Operation for Speed Control of BLDC Motor under Load Condition.

The increasing staircase operation of the BLDC motor under 2Nm loaded condition is given in figure 5.4 indicate the operation of speed control with staircase mechanism.The use staircase is variable driver application with the different reference speed.To improve the performance of speed with in different reference speed using by stair case mechanism.

The simulation result is shown figure 5.4b in the staircase mechanism the maximum current

value is 210A for changing the slope of the reference signal and the time interval between 0.5 sec to 1.5 sec the current value is 100A.The phase current increase with the change of the reference speed slope.

The simulation result is shown in the figure5.4c indicate the back emf of the BLDC motor is increased with reference speed and the simulation result is shown in the figure 5.4d show that the generates the maximum possible motor torque is 20Nm. When step speed increase command is obtained, the motor increases torque by increasing phase current.

### 5.1.4 Speed reversal of BLDC Motor

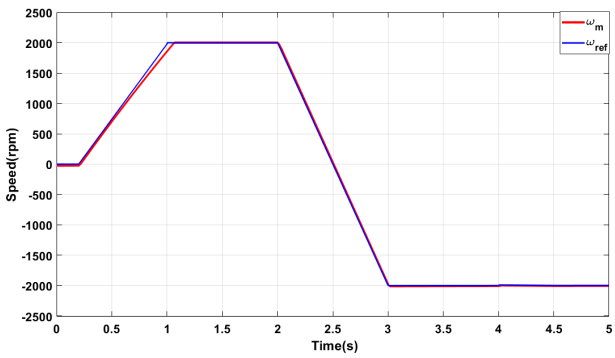


(a) Motor speed

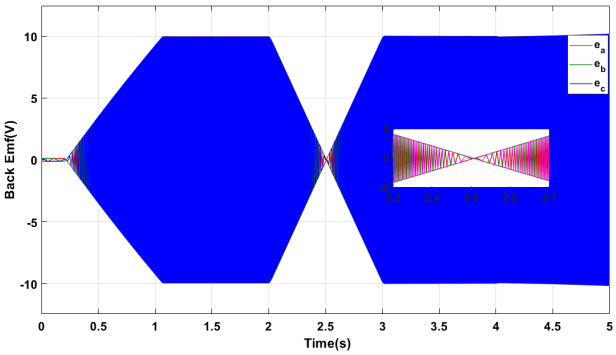


(b) Back Emf

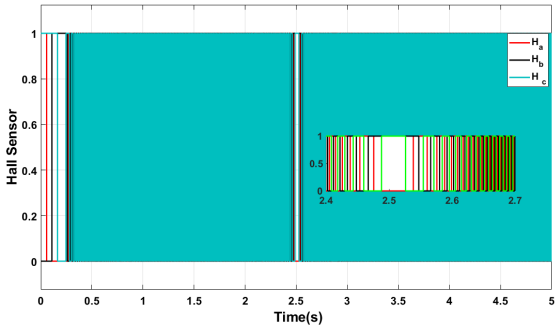


(c) Hall Sensor

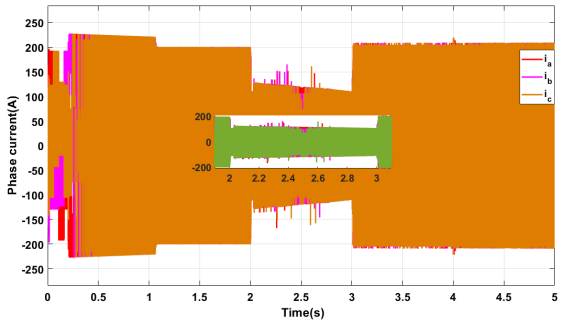


(d) phase current

Figure (5.5) Under Load the Operation of Motor Speed,Hall Sensor, Back Emf ,and Phase Current For Braking Operation.

As shown in the figure 5.5 show that the simulation result of the speed reversal operation is examined under $10Nm$ loaded conditions based on four quadrant operation is studied. Braking operation is activating the drive system for an electric vehicle.

The simulation result shown in the figure 5.5a shows that the speed reversal for braking operation during this the braking operation start at time 2.5 seconds.The current and the back emf is decreased for the braking operation at time t=2.5sec.At first the motor is operated in forwarding motoring mode.When the speed reversal command is given to the motor

undergoes braking operation is starting in the forward direction with speed tending to zero and starts rotating in the reverse direction.

The simulation result is shown in figure 5.5b show that the backemf wave form during the braking operation. In this simulation result indicate the magnitude of the back emf is increases until the steady-state is reached and in the braking mode back emf goes to decreasing up to zero.The figure shows the changeover of back Emf from braking mode to motoring mode.In the motoring mode the operation the back-emf and phase current both are increase.In case of braking mode the back emf become decrease to zero but phase current is decrees but not zero.
The simulation result in the figure 5.5c demonstrates that the variation of rotor position(Hall sensor) of the BLDC motor.When the motor is changing from forward to breaking operation at time 2.5 seconds.The simulation result on the zoom section indicate the hall sensor is operate Ha and Hc operate on(1) mode where us the Hb is off(0)mode during braking operation mode.

## 5.2 Tracking Performance Comparisons of PI and LQG Controller Under No-load,Constant Load and Time varying Load Torque

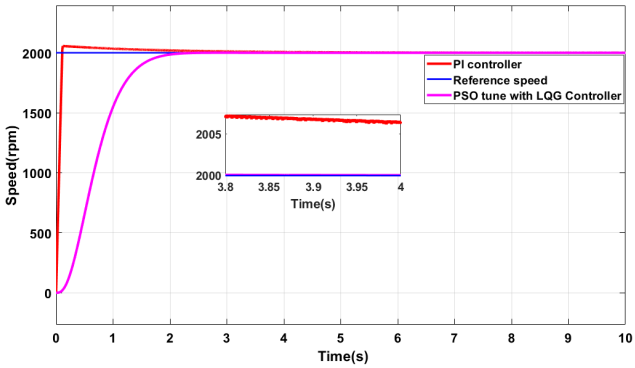


(a) Speed tracking performance of a constant reference under No-load

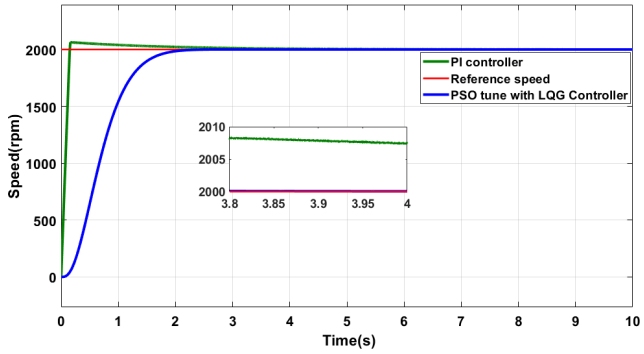


(b) Speed tracking performance under 5Nm torque load.

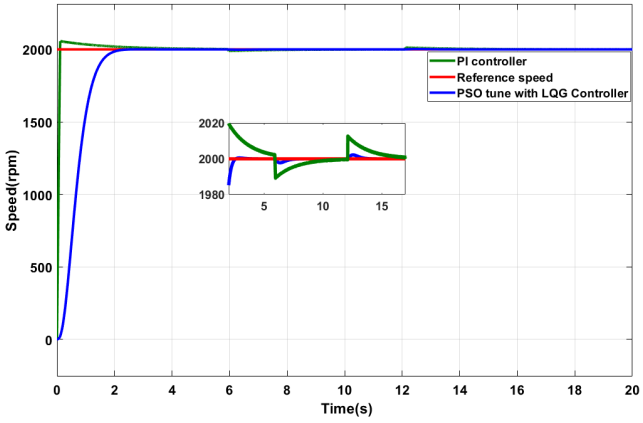


(c) Speed tracking performance under Time varying Load Torque

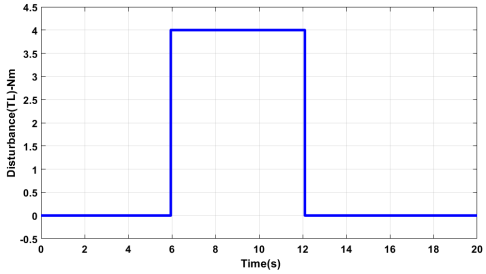


(d) Input Disturbance Load Torque

Figure (5.6) Performance comparison of LQG and PI speed controller

Figures 5.6 show that the simulation results for the comparison PI and PSO-LQG controller for the speed control of the BLDC motor.A comparison of the driving behavior using PI and PSO-LQG controller for speed control is performed under load ,time vary load ,and no-load conditions.

The simulation results are shown in the figure 5.6a show that the speed performance of the PSO-LQG controller and PI controller under no-load condition. The transient performance criteria of the PSO-LQG controller rise time,overshoot, and setting time is 0.9937 seconds,0.505%,and 1.98 seconds respectively and the PI controller rise time,overshoot, and setting time is 0.0858 seconds,2.577%,and 2.87 seconds respectively.In the zoom section show that the tracking performance of PSO-LQG controller perfect tracking for the reference speed at 2000RPM for the time interval between at t $3.8-4$ seconds time.For the same time interval the PI controller is not tracking the reference speed that means the actual speed of the PI controller is greater than reference speed.Then to conclude that the PSO-LQG controller is better performance speed tracking than PI controller under no-load condition .

The simulation result shown in figure 5.6b show the Speed response of the BLDC at 2000rpm under load(TL =5Nm) using PI controller and PSO-LQG controller.The Speed response based on the transient response is a maximum percent overshoot of 5%, the rise time of 0.0634 seconds,and settling time of 5 seconds for PI controller.And also PSO-LQG controller has less overshot of 1.09%, the rise time is 1.656 second and the setting time becomes 2.2 seconds.In the zoom section indicate the comparison between the PSO- LQG controller and PI controller for speed tracking it show that the PSO-LQG controller is better speed tracking performance than PI controller under load condition.

The simulation result shown in the figure 5.6c indicates the comparison of PSO-LQG and PI controller using speed tacking application for BLDC motor under Time-varying Load Torque. It show that the effect of disturbance in the speed tracking of the BLDC motor for the time interval between $6-12$ seconds.The tracking performance of the motor adds the pulse signal of the load torque disturbance for $6-12$seconds the magnitude is 4. Then to see the effect of motor performance become oscillation for the $6-12$ seconds for PSO-LQG controller then the controller reject the disturbance up to 12 second after that the motor tacking in the reference speed. In the PI controller the performance of speed tacking oscillation happens up to 15 seconds then disturbance band rejection start 15 second after that the motor tracking with in reference speed.Finally the simulation results show that the PSO-LQG controller has better band disturbance rejection than the PI controller.Then PSO-LQG controller has better tracking performance than the PI controller under time varying load.

# Chapter 6

# Conclusion and Future Works

## 6.1 Conclusion

In this thesis modeling and designing of PSO tune LQG controller-based of BLDC using MATLAB software to overcome the tracking performance of speed control for different speeds and to apply disturbances have been investigated. The speed control of BLDC motors is a vast developing area as it finds its applications in military, aerospace, electric vehicles application, and so on. A detailed research review has been conducted to identify the research gap that exists in this field and the implementation of the LQG controller speed controller with its coefficients of weights(the gain ) optimized by PSO to make the BLDC motor performance of the LQG controller against load disturbances and reference changes are proposed.

The speed control of the BLDC motor has been modeled in MATLAB /SIMULINK and while the simulation model of the BLDC motor includes several sub-blocks like the reference current generator, voltage equations block torque equation block, and hall sensor block, which also contains the inverter bock, the controller model, optimization technique, and switching logic control. It is described by chapter three and chapter four. Chapter three consists of the modeling, reference generator, and the dynamic model of electrical and mechanical systems. In chapter four describe the modeling of the controller and optimization technique.

The controller design requires the state-space model. From the linearization model of the BLDC motor to find the state feedback gain and the Kalman filter based on the LQR and LQE controller respectively. The speed control of the BLDC motor has been designed with an LQG controller with its coefficients of weights optimized by PSO for achieving speed tracking performance. For comparison purposes, a PI speed controller has been designed with its gains optimized by the transfer function method.

A PSO that tunes the gains of the LQG controller was developed according to the BLDC drive system characteristic, which can adjust the LQG controller parameters online according to the speed error dynamic model. As is discussed in chapter five the simulation result shows the proposed controller mechanism has a very good performance in terms of overshoot minimization, rise time, and setting time than the conventional PI controller methods. From the no-load test, the simulation results show that the LQG controller has a more significant overshoot reduction (by 0.505% and 2.577% compared to PSO tune LQG controller and PI controllers respectively and a good transient response with a rise time of 0.9937 seconds, settling time 1.95 seconds and the steady-state speed error percentage of 0.023% has been achieved. While in the case of the load test the steady-state error percentage is increased to 0.034%. Whereas, the LQG control has a 1.656 rise time,2.2 sec settling time, and overshoot 1.09% for 5 Nm torque. The performance of the PSO tune LQG controller of BLDC was analyzed in terms of speed tracking capability, rotor position(hall sensor), phase current, Back EMF, high and low-speed behavior, the step response of drive with speed reversal, and sensitivity to motor parameter uncertainty. Generally, the system also gives good performance at no load and loaded conditions. Hence, it can work with different load torque conditions and with parameters variation.

To design and model, the electric vehicle depends upon choosing the appropriate motor classification based on the carrying load. The dynamics of vehicles are considered to be the choice of the appropriate electric motor that will provide the required power, torque, for traction. Choosing the right rating also helps in using the right size electric motor, as the size of the motor depends on the rating as the function of the electric vehicle application.

## 6.2 Future Works

The proposed future work would thereby enhance the motor speed-torque characteristics performance up to wide range speed using flux weakening in the wide speed range.

To use the BLDC motor for traction drive for EVs, research on optimization should follow the limits discussed the power rating and rating torque.The proposed future to adapt the vehicle modeling and BLDC motor modeling with in hardware implementation and to analysis the performance with in experiment results.

# Appendices

# Appendix A

# Controller Design model Approach

## A.1 LQG Control Design

To design the LQG Controller the plant model will change the state-space model the BLDC motor state space represents to identify the state, input, and output from this the state variable is speed and current, the input is a voltage of the system and the output is the speed of the BLDC motor .Then from the modeling BLDC motor in above equation 3.7 and 3.12 to convert the state space representation for one phase is:

$$\begin{aligned} v_a &= Ri_a + L\frac{di_a}{dt} + e_a \\ v_b &= Ri_b + L\frac{di_b}{dt} + e_b \\ v_c &= Ri_c + L\frac{di_b}{dt} + e_c \\ T_e &= J\frac{d\omega_m}{dt} + B\omega_m + T_L \end{aligned} \tag{A.1}$$

Then from above equationA.1 rearranging differential equation as follow:

$$\begin{aligned} \frac{di_a}{dt} &= \frac{v_a}{L} - \frac{Ri_a}{L} - \frac{e_a}{L} \\ \frac{di_b}{dt} &= \frac{v_b}{L} - \frac{Ri_b}{L} - \frac{e_b}{L} \\ \frac{di_c}{dt} &= \frac{v_c}{L} - \frac{Ri_c}{L} - \frac{e_c}{L} \\ \frac{d\omega_m}{dt} &= \frac{T_e}{J} - \frac{B}{J}\omega_m - \frac{T_L}{J} \end{aligned} \tag{A.2}$$

Where $e_a = e_b = e_c = K_b\omega_m$ and $T_e = K_t(i_a + i_b + i_c)$ to substitute this value from above equationA.3 will be:

$$\begin{aligned}
\frac{di_a}{dt} &= \frac{1}{L}v_a - \frac{R}{L}i_a - \frac{K_b}{L}\omega_m \\
\frac{di_b}{dt} &= \frac{1}{L}v_b - \frac{R}{L}i_b - \frac{K_b}{L}\omega_m \\
\frac{di_c}{dt} &= \frac{1}{L}v_c - \frac{R}{L}i_c - \frac{K_b}{L}\omega_m \\
\frac{d\omega_m}{dt} &= \frac{K_t}{J}i_a + \frac{K_t}{J}i_b + \frac{K_t}{J}i_c - \frac{B}{J}\omega_m - \frac{T_L}{J}
\end{aligned} \tag{A.3}$$

The state space represent for the BLDC motor is:

$$\begin{bmatrix} \dot{i}_a \\ \dot{i}_b \\ \dot{i}_c \\ \dot{\omega}_m \end{bmatrix} = \begin{bmatrix} \frac{-R}{L} & 0 & 0 & \frac{-K_b}{L} \\ 0 & \frac{-R}{L} & 0 & \frac{-K_b}{L} \\ & 0 & 0 & \frac{-R}{L} \quad \frac{-K_b}{L} \\ & \frac{K_t}{J} & \frac{K_t}{J} & \frac{K_t}{J} \quad \frac{-B}{J} \end{bmatrix} \begin{bmatrix} i_a \\ i_b \\ i_c \\ \omega_m \end{bmatrix} + \begin{bmatrix} \frac{1}{L} & 0 & 0 & 0 \\ 0 & \frac{1}{L} & 0 & 0 \\ 0 & 0 & \frac{1}{L} & 0 \\ 0 & 0 & 0 & \frac{1}{J} \end{bmatrix} \begin{bmatrix} V_a \\ V_b \\ V_c \\ T_L \end{bmatrix}$$
$$y = \begin{bmatrix} 0 & 0 & 0 & 1 \end{bmatrix} \begin{bmatrix} i_a \\ i_b \\ i_c \\ \omega_m \end{bmatrix} \tag{A.4}$$

The state space representation of one phase for BLDC at$TL = 0$ is:

$$\begin{bmatrix} \dot{\omega}_m \\ \dot{i}_a \end{bmatrix} = \begin{bmatrix} \frac{-B}{J} & \frac{K_t}{J} \\ \frac{-K_b}{L} & \frac{-R}{L} \end{bmatrix} \begin{bmatrix} \omega_m \\ i_a \end{bmatrix} + \begin{bmatrix} 0 \\ \frac{1}{L} \end{bmatrix} U$$
$$y = \begin{bmatrix} 1 & 0 \end{bmatrix} \begin{bmatrix} \omega_m \\ i_a \end{bmatrix} \tag{A.5}$$

Then to substitute the value of the motor parameter for above table 4.1 in chapter four, i.e $R = 0.95, L = 0.0014, K_b = 9.9484, B = 0.00001, K_t = 0.095$ and $J = 0.0019$ the state space model numerically is:

$$\begin{bmatrix} \dot{\omega_m} \\ \dot{i_a} \end{bmatrix} = \begin{bmatrix} -0.005 & 50 \\ -6908.6 & -659.72 \end{bmatrix} \begin{bmatrix} \omega_m \\ i_a \end{bmatrix} + \begin{bmatrix} 0 \\ 694.4 \end{bmatrix} U$$
$$y = \begin{bmatrix} 1 & 0 \end{bmatrix} \begin{bmatrix} \omega_m \\ i_a \end{bmatrix} \tag{A.6}$$

Let $X_1$=$\omega$ and $X_2$ =$i$ from the above equation becomes:

$$\begin{bmatrix} \dot{X_1} \\ \dot{X_2} \end{bmatrix} = \begin{bmatrix} -0.005 & 50 \\ -6908.6 & -659.78 \end{bmatrix} \begin{bmatrix} X_1 \\ X_2 \end{bmatrix} + \begin{bmatrix} 0 \\ 694.4 \end{bmatrix} u$$
$$y = \begin{bmatrix} 1 & 0 \end{bmatrix} \begin{bmatrix} X_1 \\ X_2 \end{bmatrix} \tag{A.7}$$

**Error dynamic modeling**

$$e(t) = \omega_{ref} - \omega_{actual} \tag{A.8}$$

where $\omega_{ref}$ is the reference speed ,$\omega_{actual}$ is the actual speed and $e(t)$ is the error value of reference speed compare to actual speed. then the reference speed is assume constant. the error derivative value become :

$$\dot{e}(t) = -\dot{\omega}_{ref} - \dot{\omega}_{actual} \tag{A.9}$$

from the above equationA.9 the reference is constant its derivative is zero then the finally error become:

$$\dot{e}(t) = -\dot{\omega}_{actual} \tag{A.10}$$

The state of BLDC motor output is speed is symbol by $x_1$ i.e the actual speed is same as for the output speed of BLDC. then to calculate the error dynamic model state for BLDC:

$$\begin{aligned} e(t) &= \omega_{ref} - \omega_{actual} = \omega_{ref} - x_1 = z_1 \\ \dot{e}(t) &= -\dot{\omega}_{actual} = \dot{z_1} = -\dot{x_1} = z_2 \end{aligned} \tag{A.11}$$

Then the error dynamic become

$$\begin{aligned} \dot{z_2} &= -\ddot{x_1} \\ \dot{z_2} &= 0.005\dot{x_1} - 50\dot{x_2} \end{aligned} \tag{A.12}$$

then to substitute the value of $\dot{x_2}$ from above equationA.7 to get:

$$\begin{aligned} \dot{z_1} &= z_2 \\ \dot{z_2} &= -345433z_1 - 659.785z_2 + 345433\omega_{ref} + 34720u \end{aligned} \tag{A.13}$$

$$\begin{aligned} \begin{bmatrix} \dot{z_1} \\ \dot{z_2} \end{bmatrix} &= \begin{bmatrix} 0 & 1 \\ -345433 & -659.78 \end{bmatrix} \begin{bmatrix} z_1 \\ z_2 \end{bmatrix} + \begin{bmatrix} 0 & 0 \\ 345433 & 34720 \end{bmatrix} \begin{bmatrix} \omega_{ref} \\ u \end{bmatrix} \\ y &= \begin{bmatrix} 1 & 0 \end{bmatrix} \begin{bmatrix} z_1 \\ z_2 \end{bmatrix} \end{aligned} \tag{A.14}$$

## A.2 Simulink model of LQG controller

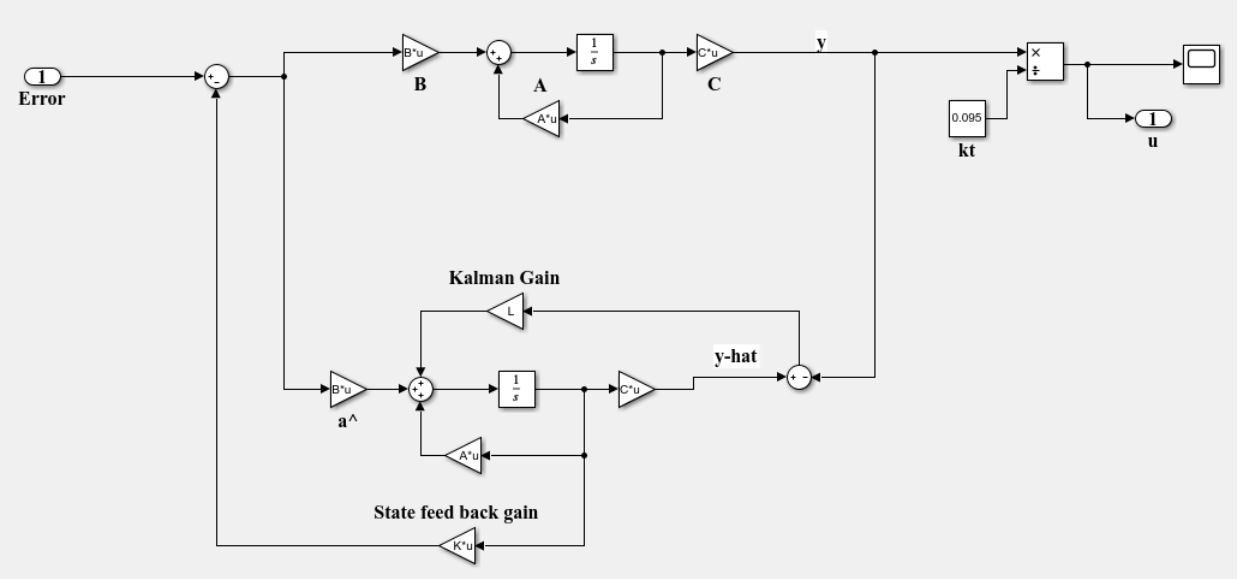


Figure (A.1) Simulink model of LQG controller based on the state space model

From above figureA.1 shows the LQG controller design to represent the state space modeling of system.In this system the in put become the error and the out put is control signal.

$$\begin{aligned} U &= -Kx \\ U &= \begin{bmatrix} -K_1 & -K_2 \end{bmatrix} \begin{bmatrix} z_1 \\ z_2 \end{bmatrix} \end{aligned} \tag{A.15}$$

The state space equation for

$$\dot{x} = Ax(t) + Bu(t) \tag{A.16}$$

Then to substitute equation A.15 in toA.16 become:

$$\begin{aligned} \dot{z_1} &= z_2 \\ \dot{z_2} &= -345433z_1 - 659.78z_2 + 34720(k_1 z_1 - k_2 z_2) \\ y &= X_1 \end{aligned} \tag{A.17}$$

Then equationA.17 becomes:

$$\begin{aligned} \dot{z_1} &= z_2 \\ \dot{z_2} &= (-345433 - 34720k_1)z_1 + (-659.78 - 34720k_2)z_2 \\ y &= X_1 \end{aligned} \tag{A.18}$$

Finally the equation A.18 is represent in LQG MATLAB/SMULINK below figure A.2

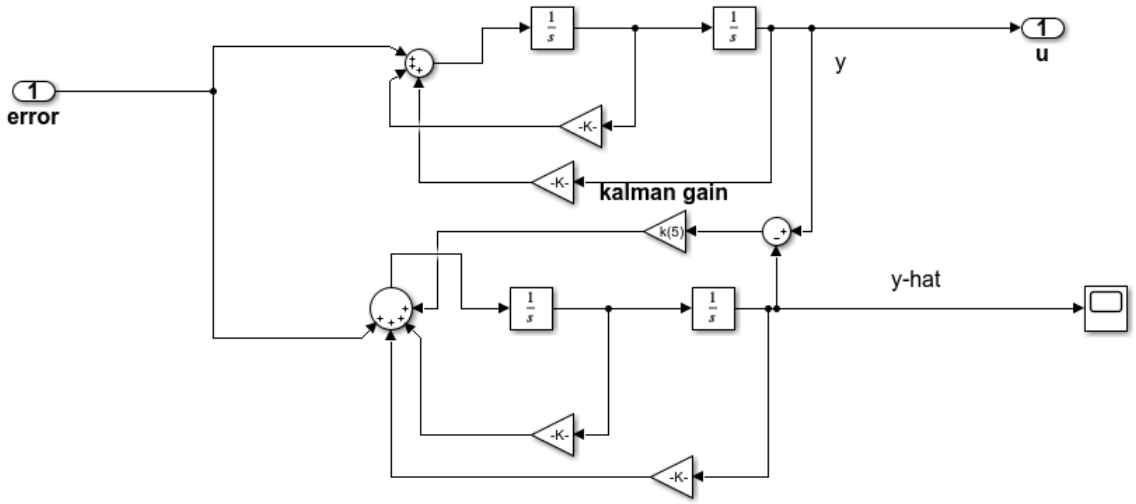


Figure (A.2) LQG MATLAB/SMULINK Model

# Appendix B

# Hysteresis current Simulink block for BLDC motor model

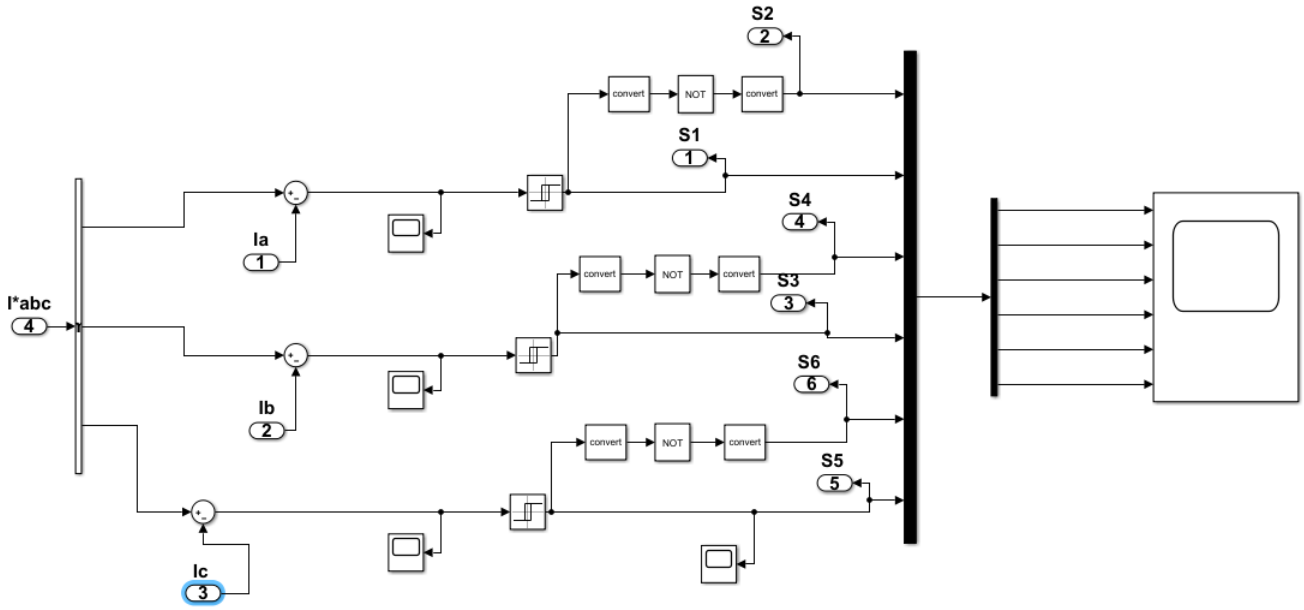


Figure (B.1) Hysteresis current Controller

The reference current generator is determine by three phase reference phase currents $i_a^*, i_b^*$and $i_c^*$) of the BLDC motor regard to the magnitude of reference current $i_{ref}$then to calculate the magnitude of reference current ($i_{ref}$) based on the hall sensor(rotor position)($\theta_r$) is.

$$i_{ref} = \frac{T_{ref}}{k_t} \tag{B.1}$$

## B.1 Ideal VSI

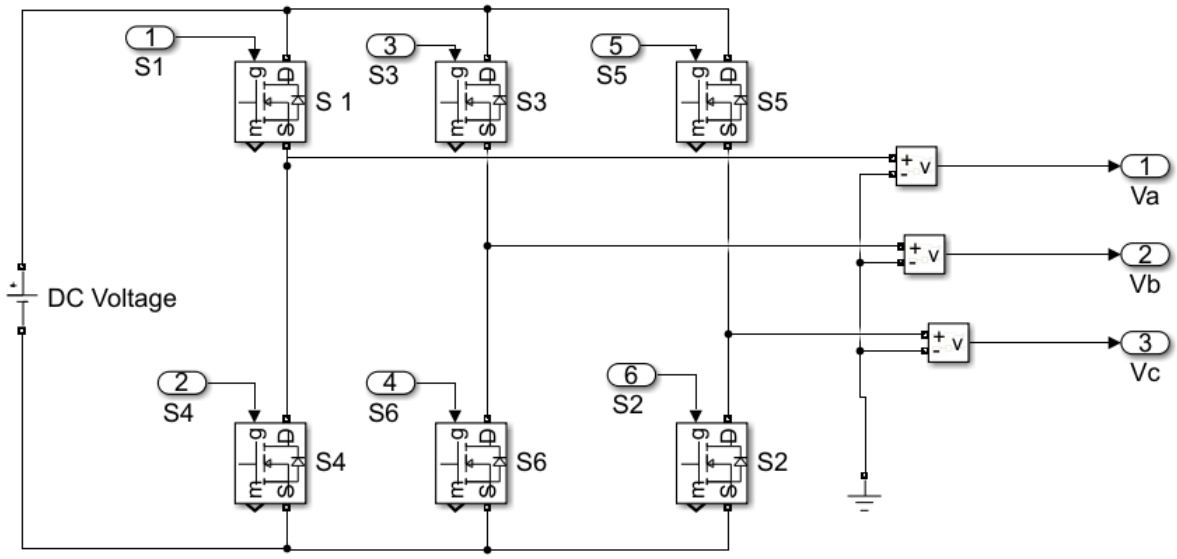


Figure (B.2) Ideal VSI Block

# Appendix C

# Program for Particle Swarm Optimization

```
clc                          %to clear the command window
clear                        %to clear the work space
%%problem settings
LB=[1 1 1 1 1] ;              %Lower bound
UB=[10 10 10 10 10];          %Upper bound
fitness=@LQG;                 %Fitness function absolute integral error
%%algorithem parameters
PO=10 ;                        %Population size
T=5;                          %No of iteration
W=0.8;                        %Inertia weight
C1=1.5;                       %Acceleration factor
C2=1.5;                       %Acceleration factor

%%parameter swarm opimization
f=NaN(Np,1)% vector to store fitness function value of population
bestfititer=NaN(T+1,1)
D=length(LB);%no of decsition variablrs in the population
P=repmat(LB,Np,1)+repmat((UB-LB),Np,1).*rand(Np,D)%generation of initial position of the
    population
v=repmat(LB,Np,1)+repmat((UB-LB),Np,1).*rand(Np,D)%generation of initial velocity of the
    population
for p=1:Np
    f(p)=fitness(P(p,:))%evaluate the fitness function of the initial population
end

pbest=P%initialize the personal best position
f_pbest=f;%initialize fitness of  the personal best solution
[f_gbest,ind]=min(f_pbest);%determine the best objective fitness function value
gbest=P(ind,:);%determine the golbal best  solution
```

```
bestfititer(1)=f_gbest;
for t=1:T
    for p=1:Np
        v(p,:)=w*v(p,:)+c1*rand(1,D).*(pbest(p,:)-P(p,:))+c2*rand(1,D).*(gbest-P(p,:)); %
            determinr new velecity
        P(p,:)=P(p,:)+v(p,:);  %update new position
        P(p,:)=max(P(p,:),lb);%bounding violating variables to lower bound
        P(p,:)=min(P(p,:),ub);%bounding violating variables to upper bound
        f(p)=prob(P(p,:));% determine fitness of the new solution
        if f(p)<f_pbest(p)
            f_pbest(p)=f(p);%updating fitness function of personal bestsolution
            pbest(p,:)=P(p,:);%updating pbest solution
            if f_pbest(p)<f_gbest
                f_gbest=f_pbest(p);%updating fitness value of the best solution
                gbest=pbest(p,:);%updating  the best solution
            end
        end
    end
    bestfititer(t+1)=f_gbest;
    disp(['iteration',num2str(t),':best fitness=',num2str(bestfititer(t+1))])
    k
end
best_fitness=f_gbest
bestsol=gbest
```

# Appendix D

# Electrical Vehicle Modeling

### D.0.1 Analysis of Aerodynamics Dragging force versus speed of the car

```
clear all;
m=1500;            % mass of the Vehicle
g=9.81;
a=2.22;            % acceleratin in m/s^2
r=0.48;            % Radius of the wheel
K_friction=0.01;  % Coefficient of friction for asphalt road
F_tot=0;
v=22.22;           % speed of the car in m/s
Tot_effcen.M=0.85;
Airp=1.2;          % air density Kg/m^3
Af=2.43;           % area in m^2
vo=0;              % air velocity in m/s
CA=0.26;           % drag coefficient
%Initial condition
Vkph=0;
Vkph1=0;
d_Vkph=1e-2;        %unit step increment
Vkph_final=80;      % final value in km/hr.
x=1;
n=1;
while(Vkph<Vkph_final),
Vmps=Vkph*(1000/3600);
Fady=0.5*Airp*CA*Af*(Vmps+vo)^2;
if Vkph<=80*d_Vkph;
statfric=0.2;
else
statfric=0;
end
F_tot=m*g*(K_friction+statfric)+Fady+m*a;   % Total force(Nm)
Power=F_tot*Vmps/0.85; % Required input power (Watt)
Torque=(Power*r/Vmps);    % Nm
```

```
Vkph=Vkph+d_Vkph;
Vkph1=Vkph1+d_Vkph;
if x>0,
F_totn(n)=F_tot;
Torquen(n)=Torque;
Powern(n)=Power/1000; %Power in KW
Fady(n)=Fady;
Vkphn(n)=Vkph;
n=n+1;
x=1;
end
x=x+1;
end
plot(Vkphn,Fady,'r','LineWidth',2);
axis([0 80 0 188]);
grid
xlabel('Speed of the car (Km/hr)')
ylabel('Aerodynamic (Drag) Resistance Force (N)')
```

### D.0.2 Consumed power versus speed of the vehicle

```
m=1500;          % mass of the Vehicle
fric=0.01;
g=9.81;
a=1.8;            % acceleratin in m/s^2
r=0.48;           % Radius of the wheel
K_friction=0.01;  % Coefficient of friction
F_tot=0;
v=22.2;           % speed of the car in m/s
Tot_effcen.M=0.85;
Adnsty=1.2;      %air density Kg/m^3
Af=2.43;         %area in m^2
vo=0;            %air velocity in m/s
CA=0.26;         % drag coefficient
%Initial condition
Vkph=0;
Vkph1=0;
d_Vkph=1e-2;     %unit step increment
Vkph_final=100;  %final value in km/hr.
x=1;
n=1;
while(Vkph<Vkph_final),
Vmps=Vkph*(1000/3600);
Fadyna=0.5*Adnsty*CA*Af*(Vmps+vo)^2;
if Vkph<=100*d_Vkph;
statfric=0.2;
else
statfric=0;
end
F_tot=m*g*(K_friction+statfric)+Fadyna+m*a;  % Total force(Nm)
Power=F_tot*Vmps/0.95;                      % Required input power (Watt)
```

```
Torque=(Power*r/Vmps);                          % Nm
Vkph=Vkph+d_Vkph;
Vkph1=Vkph1+d_Vkph;
if x>0,
F_totn(n)=F_tot;
Torquen(n)=Torque;
Powern(n)=Power/1000;                        %Power in KW
Fadynan(n)=Fadyna;
Vkphn(n)=Vkph;
n=n+1;
x=1;
end
x=x+1;
end
plot(Vkphn,Powern,'r','LineWidth',2);
set(gca,'FontSize',12)
axis([0 100 0 80]);
grid
xlabel('Speed of the of the car(Km/hr)')
ylabel('Power (KW)')
```

# Appendix E

# MATLAB/SMULINK Model of the BLDC motor

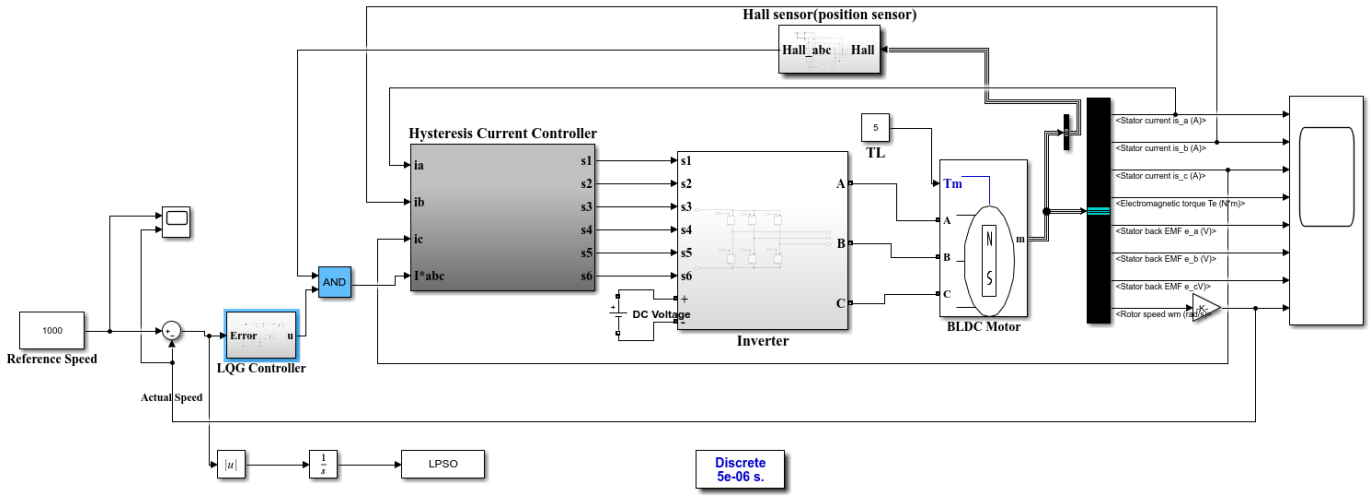


Figure (E.1) Over all MATLAB/SMULINK Model of the BLDC motor

# Bibliography


[1] Vladimir Hubik, Martin Sveda, and Vladislav Singule. "On the development of BLDC motor control run-up algorithms for aerospace application". In: *2008 13th international power electronics and motion control conference*. IEEE. 2008, pp. 1620–1624.

[2] Xiaoyan Huang et al. "A single sided matrix converter drive for a brushless DC motor in aerospace applications". In: *IEEE Transactions on Industrial Electronics* 59.9 (2011), pp. 3542–3552.

[3] A Tashakori, M Ektesabi, and N Hosseinzadeh. "Modeling of bldc motor with ideal back-emf for automotive applications". In: *Proceedings of the World Congress on Engineering*. Vol. 2. 2011, pp. 6–8.

[4] Mohamed Z Youssef. "Design and performance of a cost-effective BLDC drive for water pump application". In: *IEEE Transactions on Industrial Electronics* 62.5 (2014), pp. 3277–3284.

[5] WAN FAIZURA WAN TARMIZI. "MODELLING AND CONTROL OF MULTI-FINGERED ROBOT HAND USING INTELLIGENT TECHNIQUES". PhD thesis. Universiti Teknologi PETRONAS, 2014.

[6] Pushek Madaan. "Brushless dc motors–part i: Construction and operating principles". In: *Cypress Semiconductor* 11 (2013).

[7] James Larminie and John Lowry. *Electric vehicle technology explained*. John Wiley & Sons, 2012.

[8] Andrew Pennycott et al. "Enhancing the energy efficiency of fully electric vehicles via the minimization of motor power losses". In: *2013 IEEE international conference on systems, man, and cybernetics*. IEEE. 2013, pp. 4167–4172.

[9] Jian-Bo He, Qing-Guo Wang, and Tong-heng Lee. "PI/PID controller tuning via LQR approach". In: *Chemical Engineering Science* 55 (2000), pp. 2429–2439.

[10] Mehdi Nasri, Hossein Nezamabadi-Pour, and Malihe Maghfoori. "A PSO-based optimum design of PID controller for a linear brushless DC motor". In: *World Academy of Science, Engineering and Technology* 26.40 (2007), pp. 211–215.

[11] Gwo-Ruey Yu and Rey-Chue Hwang. "Optimal PID speed control of brush less DC motors using LQR approach". In: *2004 IEEE International Conference on Systems, Man and Cybernetics (IEEE Cat. No. 04CH37583)*. Vol. 1. IEEE. 2004, pp. 473–478.

[12] MA Aravind, Niranjan Saikumar, and NS Dinesh. "Optimal position control of a DC motor using LQG with EKF". In: *2017 international conference on mechanical, system and control engineering (ICMSC)*. IEEE. 2017, pp. 149–154.

[13] AA Bature, Mustapha Muhammad, and Auwalu M Abdullahi. "Position control of a DC motor: An experimental comparative assessment between fuzzy and state feedback controller". In: *ARPN Journal of Engineering and Applied Sciences* 8.12 (2013), pp. 984–987.

[14] G Prasad et al. "Modelling and Simulation Analysis of the Brushless DC Motor by using MATLAB". In: *International journal of innovative technology and exploring engineering (IJITEE)* 1.5 (2012), pp. 27–31.

[15] Prakash Salawria, Rakesh Singh Lodhi, and Pragya Nema. "Implementation of PSO-based optimum controller for speed control of BLDC motor". In: *International Journal of Electrical, Electronics and Computer Engineering* 6.1 (2017), pp. 104–109.

[16] Dian-sheng Sun, Xiang Cheng, and Xu-qiang Xia. "Research of Novel Modeling and Simulation Approach of Brushless DC Motor Control System". In: *2010 International Conference on E-Product E-Service and E-Entertainment*. IEEE. 2010, pp. 1–5.

[17] Bapayya Naidu Kommula and Venkata Reddy Kota. "Performance evaluation of hybrid fuzzy pi speed controller for brushless dc motor for electric vehicle application". In: *2015 Conference on power, control, communication and computational technologies for sustainable growth (PCCCTSG)*. IEEE. 2015, pp. 266–270.

[18] Nasser Hashemnia and Behzad Asaei. "Comparative study of using different electric motors in the electric vehicles". In: *2008 18th International Conference on Electrical Machines*. IEEE. 2008, pp. 1–5.

[19] Milan Brejl, Michal Princ, and Pavel Sustek. "BLDC Motor with Hall Sensors and Speed Closed Loop, Driven by eTPU on MPC5554". In: (2006).

[20] CS Vishnu and Riya Mary Francis. "Speed Control of BLDC Motor by Using Tuned Linear Quadratic Regulator". In: *Int. J. Sci. Eng. Res* 3.8 (2015), pp. 36–40.

[21] JM Ahmed. "Optimal LQG Controller Based on Genetic Algorithm Technique For Speed Control of CD Motor". In: *International Journal of Engineering and Innovative Technology (IJEIT) Volume* 7 (2017).

[22] YS Jeon et al. "A new simulation model of BLDC motor with real back EMF waveform". In: *COMPEL 2000. 7th Workshop on Computers in Power Electronics. Proceedings (Cat. No. 00TH8535)*. IEEE. 2000, pp. 217–220.

[23] Shivraj S Dudhe and Archana G Thosar. "Mathematical modelling and simulation of three phase BLDC motor using MATLAB/Simulink". In: *International Journal of Advances in Engineering & Technology* 7.5 (2014), p. 1426.

[24] A Purna Chandra Rao, YP Obulesh, and Ch Sai Babu. "Mathematical modeling of BLDC motor with closed loop speed control using PID controller under various loading conditions". In: *arpn journal of engineering and applied sciences* 7.10 (2012), pp. 1321–1328.

[25] M Poovizhi et al. "Investigation of mathematical modelling of brushless dc motor (BLDC) drives by using MATLAB-SIMULINK". In: *2017 International Conference on Power and Embedded Drive Control (ICPEDC)*. IEEE. 2017, pp. 178–183.

[26] Hemchand Immaneni. "Mathematical modelling and position control of brushless dc (BLDC) motor". In: *International Journal of Engineering Research and Applications* 3.3 (2013), pp. 1050–1057.

[27] Ameer L Saleh and Adel A Obed. "Speed control of brushless DC motor based on fractional order PID controller". In: *International Journal of Computer Applications* 95.4 (2014).

[28] S Rambabu. "Modeling and control of a brushless DC motor". In: *Master of Thesis In Power Control and Drives Technology, National Institute of Technology Rourkela* (2007).

[29] Mohamed Shamseldin. "Speed control of high performance brushless DC motor". PhD thesis. Thesis. 2016. Helwan University: Egypt, 2016.

[30] Vaishali Rajendra Walekar and SV Murkute. "Speed Control of BLDC Motor using PI & Fuzzy Approach: A Comparative Study". In: *2018 International Conference on Information, Communication, Engineering and Technology (ICICET)*. IEEE. 2018, pp. 1–4.

[31] Momir Stanković et al. "Fuzzy model reference adaptive control of velocity servo system". In: *Facta Universitatis, Series: Electronics and Energetics* 27.4 (2014), pp. 601–611.

[32] OĞUZ Yüksel, Hasan ERDAL, and Sezai TAŞKIN. "Design and simulation of a LQG robust controller for an electrical power system". In: *IU-Journal of Electrical & Electronics Engineering* 8.2 (), pp. 693–698.

[33] Ragnar Eide, Per Magne Egelid, Hamid Reza Karimi, et al. "LQG control design for balancing an inverted pendulum mobile robot". In: *Intelligent Control and Automation* 2.02 (2011), p. 160.

[34] K Rajeswari et al. "Extended Kalman filter for vehicle suspension system". In: *Applied Mechanics and Materials*. Vol. 573. Trans Tech Publ. 2014, pp. 317–321.

[35] Zhuoyi Chen, Zhuo Sun, and Wenbo Wang. "Design and implementation of Kalman filter". In: (2011).

[36] Sarthak Modak and Sumangal Bhaumik. "Comparative study of controllers MIMO System". In: *2020 International Conference on Computer, Electrical & Communication Engineering (ICCECE)*. IEEE. 2020, pp. 1–6.

[37] Louiza Sellami. "Simulink model of a full state observer for a DC motor position, speed, and current". In: *Proceedings of the International Conference on Modeling, Simulation and Visualization Methods (MSV)*. The Steering Committee of The World Congress in Computer Science, Computer ... 2014, p. 1.

[38] Santanu Mondal, Arunabha Mitra, and Madhurima Chattopadhyay. "Mathematical modeling and simulation of Brushless DC motor with ideal Back EMF for a precision speed control". In: *2015 IEEE International Conference on Electrical, Computer and Communication Technologies (ICECCT)*. IEEE. 2015, pp. 1–5.

[39] Dongshu Wang, Dapei Tan, and Lei Liu. "Particle swarm optimization algorithm: an overview". In: *Soft Computing* 22.2 (2018), pp. 387–408.

[40] X Xie, W Zhang, L Yang, et al. "Particle swarm optimization". In: *Control and Decision* 18 (2003), pp. 129–134.

[41] T Porselvi et al. "Selection of power rating of an electric motor for electric vehicles". In: *International Journal of Engineering Science and Computing IJESC* 7.4 (2017), pp. 6469–6472.

[42] Saurabh Chauhan. "Motor torque calculations for electric vehicle". In: *International journal of scientific & technology research* 4.8 (2015), pp. 126–127.

[43] Iqbal Husain and Mohammad S Islam. "Design, modeling and simulation of an electric vehicle system". In: *SAE transactions* (1999), pp. 2168–2176.

[44] Xiaodong Sun et al. “Analysis and design optimization of a permanent magnet synchronous motor for a campus patrol electric vehicle”. In: *IEEE Transactions on Vehicular Technology* 68.11 (2019), pp. 10535–10544.